

1

2

3 ***LEAFY maintains apical stem cell activity during shoot development in***
4 ***the fern *Ceratopteris richardii****

5

6 **Andrew R.G. Plackett^{1*}†, Stephanie J. Conway^{2*‡}, Kristen D. Hewett Hazelton², Ester H.**
7 **Rabbinowitsch¹, Jane. A. Langdale^{1\$#}, Verónica S. Di Stilio^{2§}**

8 ¹ Department of Plant Sciences, University of Oxford, South Parks Road, Oxford, OX1 3RB, UK

9 ² Department of Biology, University of Washington, Seattle, WA 98195-1800, USA

10 † Current address: Department of Plant Sciences, University of Cambridge, Downing Street,
11 Cambridge, CB2 3EA, UK.

12 ‡ Current address: Department of Organismic and Evolutionary Biology, Harvard University, 16
13 Divinity Ave., Cambridge, MA 02138, USA

14

15

16

17

18

19

20

21

22

23 *Equal contribution.

24 § Equal contribution.

25 # Corresponding author: jane.langdale@plants.ox.ac.uk

26 **ABSTRACT**

27 During land plant evolution, determinate spore-bearing axes (retained in extant bryophytes such as
28 mosses) were progressively transformed into indeterminate branching shoots with specialized
29 reproductive axes that form flowers. The LEAFY transcription factor, which is required for the first
30 zygotic cell division in mosses and primarily for floral meristem identity in flowering plants, may have
31 facilitated developmental innovations during these transitions. Mapping the LEAFY evolutionary
32 trajectory has been challenging, however, because there is no functional overlap between mosses and
33 flowering plants, and no functional data from intervening lineages. Here, we report a transgenic analysis
34 in the fern *Ceratopteris richardii* that reveals a role for LEAFY in maintaining cell divisions in the
35 apical stem cells of both haploid and diploid phases of the lifecycle. These results support an
36 evolutionary trajectory in which an ancestral LEAFY module that promotes cell proliferation was
37 progressively co-opted, adapted and specialized as novel shoot developmental contexts emerged.

38

39

40

41 **AUTHOR CONTRIBUTIONS**

42 VSD cloned the *CrLFY* coding sequences and made the RNAi constructs during a sabbatical visit to the
43 University of Oxford; ARP and EHR performed transformations in *Ceratopteris richardii* and EHR
44 maintained T₀ transgenic plants; ARP cloned the *CrLFYI* promoter, made GUS reporter constructs,
45 validated transgenic reporter lines, conducted GUS staining, and performed gel blot analysis of *CrLFY*
46 copy number; SJC and KDHH screened, validated and characterized the RNAi lines; KDHH performed
47 ontogenetic gene expression analysis; VSD performed statistical analyses; SJC conducted *in situ*
48 localization experiments; JAL performed the phylogenetic analysis; JAL & ARP wrote the first draft of
49 the paper, all authors contributed to the final version.

50

51 **ACKNOWLEDGEMENTS**

52 Work in JAL's lab was funded by an ERC Advanced Investigator Grant (EDIP) and by the Gatsby
53 Charitable Foundation. VSD's visit to JAL's lab was funded in part by NSF/EDEN IOS # 0955517.
54 Work in VSD's lab was funded by the Royalty Research Fund and Bridge Funding Program, University
55 of Washington. We thank Brittany Dean for her contribution to transgenic line screening and validation.

56

57 **COMPETING INTERESTS**

58 The authors declare that they have no competing interests

59

60 **KEYWORDS**

61 *C. richardii*, fern, *LEAFY*, *FLORICAULA*, shoot development, land plant evolution, apical cells

62

63

64

65

66 INTRODUCTION

67 Land plants are characterized by the alternation of haploid (gametophyte) and diploid (sporophyte)
68 phases within their lifecycle, both of which are multicellular (Niklas and Kutschera, 2010; Bowman et
69 al., 2016). In the earliest diverging bryophyte lineages (liverworts, mosses and hornworts) the free-
70 living indeterminate gametophyte predominates the lifecycle, producing gametes that fuse to form the
71 sporophyte. The sporophyte embryo develops on the surface of the gametophyte, ultimately forming a
72 simple determinate spore-producing axis (Kato and Akiyama, 2005; Ligrone et al., 2012). By contrast,
73 angiosperm (flowering plant) sporophytes range from small herbaceous to large arborescent forms, all
74 developing from an indeterminate vegetative shoot apex that ultimately transitions to flowering; and
75 gametophytes are few-celled determinate structures produced within flowers (Schmidt et al., 2015). A
76 series of developmental innovations during the course of land plant evolution thus simplified
77 gametophyte form whilst increasing sporophyte complexity, with a prolonged and plastic phase of
78 vegetative development arising in the sporophyte of all vascular plants (lycophytes, ferns, gymnosperms
79 and angiosperms).

80

81 Studies aimed at understanding how gene function evolved to facilitate developmental innovations
82 during land plant evolution have thus far largely relied on comparative analyses between bryophytes
83 and angiosperms, lineages that diverged over 450 million years ago. Such comparisons have revealed
84 examples of both sub- and neo-functionalization following gene duplication, and of co-option of
85 existing gene regulatory networks into new developmental contexts. For example, a single bHLH
86 transcription factor in the moss *Physcomitrella patens* regulates stomatal differentiation, whereas gene
87 duplications have resulted in three homologs with sub-divided stomatal patterning roles in the
88 angiosperm *Arabidopsis thaliana* (hereafter ‘Arabidopsis’) (MacAlister and Bergmann, 2011); class III
89 HD-ZIP transcription factors play a conserved role in the regulation of leaf polarity in *P. patens* and
90 Arabidopsis but gene family members have acquired regulatory activity in meristems of angiosperms
91 (Yip et al., 2016); and the gene regulatory network that produces rhizoids on the gametophytes of both
92 the moss *P. patens* and the liverwort *Marchantia polymorpha* has been co-opted to regulate root hair

93 formation in *Arabidopsis* sporophytes (Menand et al., 2007; Pires et al., 2013; Proust et al., 2016). In
94 many cases, however, interpreting the evolutionary trajectory of gene function by comparing lineages
95 as disparate as bryophytes and angiosperms has proved challenging, particularly when only a single
96 representative gene remains in most extant taxa – as is the case for the *LEAFY* (*LFY*) gene family (Himi
97 et al., 2001; Maizel et al., 2005; Sayou et al., 2014).

98

99 The *LFY* transcription factor, which is present across all extant land plant lineages and related
100 streptophyte algae (Sayou et al., 2014), has distinct functional roles in bryophytes and angiosperms. In
101 *P. patens*, *LFY* regulates cell divisions during sporophyte development (including the first division of
102 the zygote) (Tanahashi et al., 2005), whereas in angiosperms the major role is to promote the transition
103 from inflorescence to floral meristem identity (Carpenter and Coen, 1990; Schultz and Haughn, 1991;
104 Weigel et al., 1992; Weigel and Nilsson, 1995; Souer et al., 1998; Molinero-Rosales et al., 1999). Given
105 that *LFY* proteins from liverworts and all vascular plant lineages tested to date (ferns, gymnosperms
106 and angiosperms) bind a conserved target DNA motif, whereas hornwort and moss homologs bind to
107 different lineage-specific motifs (Sayou et al., 2014), the divergent roles in mosses and angiosperms
108 may have arisen through the activation of distinct networks of downstream targets. This suggestion is
109 supported by the observation that *PpLFY* cannot complement loss-of-function *lfy* mutants in
110 *Arabidopsis* (Maizel, 2005). Similar complementation studies indicate progressive functional changes
111 as vascular plant lineages diverged in that the *lfy* mutant is not complemented by lycophyte *LFY*
112 proteins (Yang et al., 2017) but is partially complemented by fern and (increasingly) gymnosperm
113 homologs (Maizel et al., 2005). Because *LFY* proteins from ferns, gymnosperms and angiosperms
114 recognize the same DNA motif, this progression likely reflects co-option of a similar *LFY* gene
115 regulatory network into different developmental contexts. As such, the role in floral meristem identity
116 in angiosperms would have been co-opted from an unknown ancestral context in non-flowering vascular
117 plants, a context that cannot be predicted from existing bryophyte data.

118

119 The role of *LFY* in non-flowering vascular plant lineages has thus far been hypothesized on the basis of
120 expression patterns in the lycophyte *Isoetes sinensis* (Yang et al., 2017), the fern *Ceratopteris richardii*
121 (hereafter ‘Ceratopteris’) (Himi et al., 2001) and several gymnosperm species (Mellerowicz et al.;
122 Mouradov et al., 1998; Shindo et al., 2001; Carlsbecker et al., 2004; Vázquez-Lobo et al., 2007;
123 Carlsbecker et al., 2013). These studies reported broad expression in vegetative and reproductive
124 sporophyte tissues of *I. sinensis* and gymnosperms, and in both gametophytes and sporophytes of
125 Ceratopteris. Although gene expression can be indicative of potential roles in each case, the possible
126 evolutionary trajectories and differing ancestral functions proposed for *LFY* within the vascular plants
127 (Theissen and Melzer, 2007; Moyroud et al., 2010) cannot be resolved without functional validation.
128 Here we present a functional analysis in Ceratopteris that reveals a stem cell maintenance role for *LFY*
129 in both gametophyte and sporophyte shoots and discuss how that role informs our mechanistic
130 understanding of developmental innovations during land plant evolution.

131

132 RESULTS

133 *The CrLFY1 and CrLFY2 genes duplicated recently within the fern lineage*

134 The *LFY* gene family is present as a single gene copy in most land plant genomes (Sayou et al., 2014).
135 In this regard, the presence of two *LFY* genes in Ceratopteris (Himi et al., 2001) is atypical. To determine
136 whether this gene duplication is more broadly represented within the ferns and related species (hereafter
137 ‘ferns’), a previous amino acid alignment of *LFY* orthologs (Sayou et al., 2014) was pruned and
138 supplemented with newly-available fern homologs (see Materials and Methods) to create a dataset of
139 120 sequences, ~50% of which were from the fern lineage (**Supplementary Files 1-3**). The
140 phylogenetic topology inferred within the vascular plants using the entire dataset (**Figure 1-figure**
141 **supplement 1**) was consistent with previous analyses (Qiu et al., 2006; Wickett et al., 2014). Within
142 the ferns (64 in total), phylogenetic relationships between *LFY* sequences indicated that the two gene
143 copies identified in *Equisetum arvense*, *Azolla caroliniana* and Ceratopteris each resulted from recent
144 independent duplication events (**Figure 1**). Gel blot analysis confirmed the presence of no more than
145 two *LFY* genes in the Ceratopteris genome (**Figure 1-figure supplement 2**). Given that the topology of

146 the tree excludes the possibility of a gene duplication prior to diversification of the ferns, *CrLFY1* and
147 *CrLFY2* are equally orthologous to the single copy *LFY* representatives in other fern species.

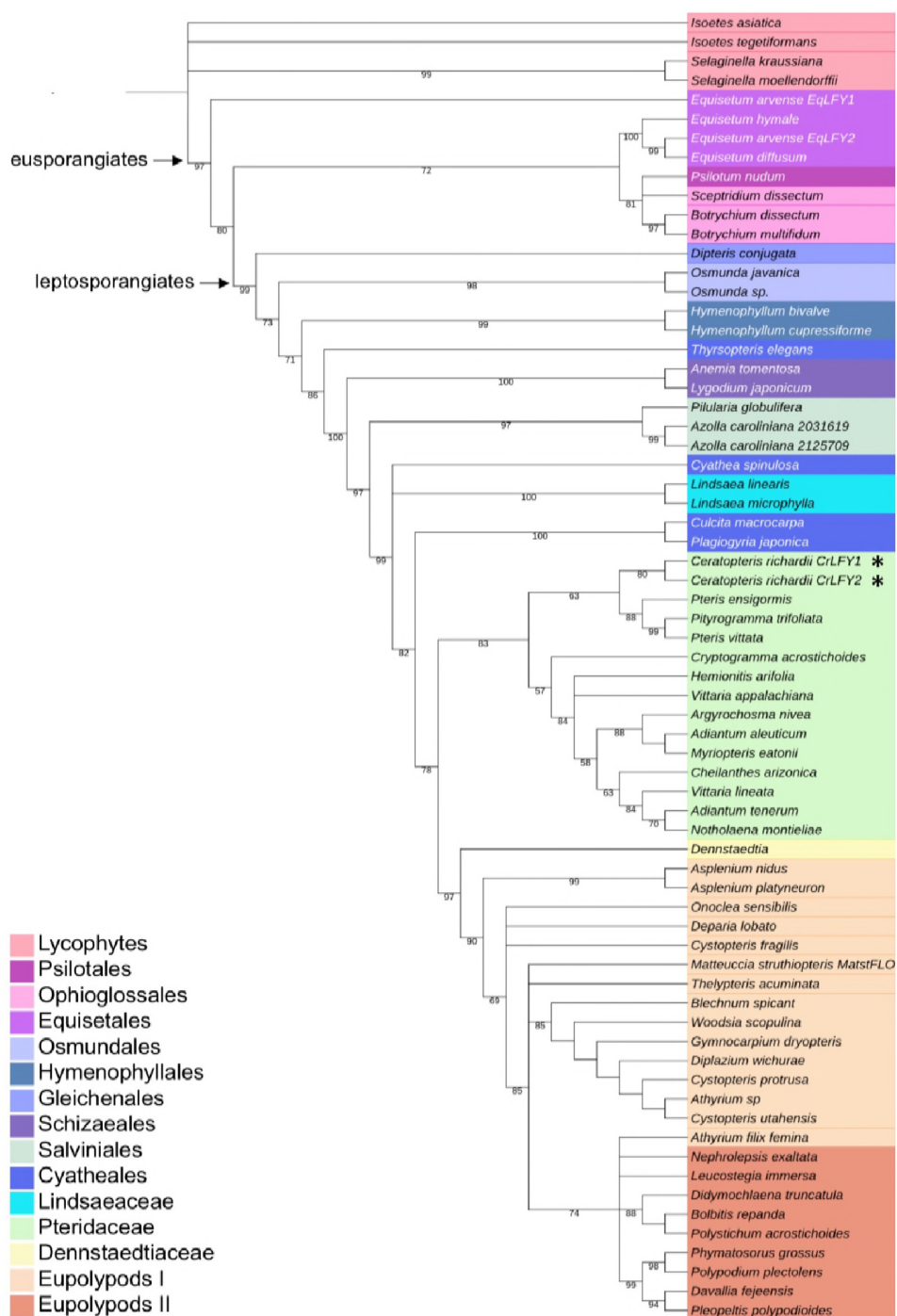


Figure 1. *CrLFY1* and *CrLFY2* arose from a recent gene duplication event.

Inferred phylogenetic tree from maximum likelihood analysis of 64 LFY amino acid sequences (see **Supplementary File 1** for accession numbers) sampled from within the fern lineage plus lycophyte sequences as an outgroup. Bootstrap values are given for each node. The tree shown is extracted from a phylogeny with representative sequences from all land plant lineages (**Figure 1-figure supplement 1**). The *Ceratopteris richardii* genome contains no more than two copies of LFY (**Figure 1-figure supplement 2**; indicated by *). Different taxonomic clades within the fern lineage are denoted by different colours, as shown. The divergence between eusporangiate and leptosporangiate ferns is indicated by arrows.

149 **CrLFY1 and CrLFY2 transcripts accumulate differentially during the Ceratopteris lifecycle**

150 The presence of two *LFY* genes in the Ceratopteris genome raises the possibility that gene activity was
151 neo- or sub-functionalized following duplication. To test this hypothesis, transcript accumulation
152 patterns of *CrLFY1* and *CrLFY2* were investigated throughout the Ceratopteris lifecycle. The sampled
153 developmental stages spanned from imbibed spores prior to germination (**Figure 2A**), to differentiated
154 male and hermaphrodite gametophytes (**Figure 2B-D**), through fertilization and formation of the diploid
155 embryo (**Figure 2E**), to development of the increasingly complex sporophyte body plan (**Figure 2F-**
156 **K**). Quantitative RT-PCR analysis detected transcripts of both *CrLFY1* and *CrLFY2* at all stages after
157 spore germination, but only *CrLFY2* transcripts were detected in spores prior to germination (**Figure**
158 **2L**). A two-way ANOVA yielded a highly significant interaction ($F(10,22) = 14.21$; $p < 0.0001$)
159 between gene copy and developmental stage that had not been reported in earlier studies (Himi et al.,
160 2001), and is indicative of differential *CrLFY1/2* gene expression that is dependent on developmental
161 stage. Of particular note were significant differences between *CrLFY1* and *CrLFY2* transcript levels
162 during sporophyte development. Whereas *CrLFY2* transcript levels were comparable across sporophyte
163 samples, *CrLFY1* transcript levels were much higher in samples that contained the shoot apex (**Figure**
164 **2F, G**) than in those that contained just fronds (**Figure 2H-K**). These data suggest that *CrLFY1* and
165 *CrLFY2* genes may play divergent roles during sporophyte development, with *CrLFY1* acting primarily
166 in the shoot apex and *CrLFY2* acting more generally.

167

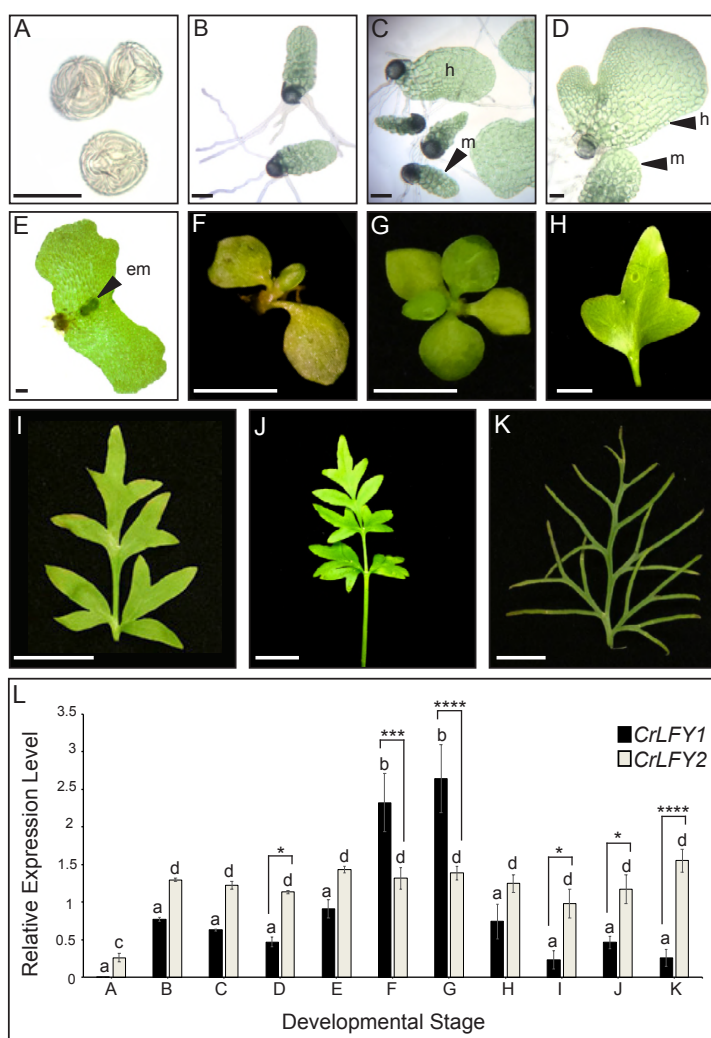


Figure 2. *CrLFY1* and *CrLFY2* are differentially expressed during the *Ceratopteris* lifecycle. A-K. Representative images of the developmental stages sampled for expression analysis in (L). Imbibed spores (A); populations of developing gametophytes harvested at 5 (B, C) and 8 (D) days after spore-sowing (DPS), comprising only males (B) or a mixture of hermaphrodites (h) and males (m) (C, D); fertilized gametophyte subtending a developing sporophyte embryo (em) (E); whole sporophyte shoots comprising the shoot apex with 3 (F) or 5 expanded entire fronds attached (G); individual vegetative fronds demonstrating a heteroblastic progression in which frond complexity increases through successive iterations of lateral outgrowths (pinnae) (H-J); complex fertile frond with sporangia on the underside of individual pinnae (K). Scale bars = 100 um (A-E), 5 mm (F-H), 20 mm (I-K). **L.** Relative expression levels of *CrLFY1* and *CrLFY2* (normalised against the housekeeping genes *CrACTIN1* and *CrTBP*) at different stages of development. $n = 3$; Error bars = standard error of the mean (SEM). Pairwise statistical comparisons (ANOVA followed by Tukey's multiple comparisons test–Supplementary File 4) found no significant difference in *CrLFY2* transcript levels between any gametophyte or sporophyte tissues sampled after spore germination ($p > 0.05$) and no significant difference between *CrLFY1* and *CrLFY2* transcript levels during early gametophyte development ($p > 0.05$) (B, C). Differences between *CrLFY1* and *CrLFY2* transcript levels were significant in gametophytes at 8 DPS ($P < 0.05$) (D). *CrLFY1* transcript levels were significantly higher in whole young sporophytes (F) and vegetative shoots (G) compared to isolated fronds (H-K) ($p < 0.05$). *CrLFY1* transcript levels in whole sporophytes and shoots were greater than *CrLFY2*, whereas in isolated fronds *CrLFY1* transcript levels were consistently lower than *CrLFY2* ($p < 0.05$). Asterisks denote significant difference (*, $p < 0.05$; **, $p < 0.01$, ***, $p < 0.001$; ****, $p < 0.0001$) between *CrLFY1* and *CrLFY2* transcript levels (Sidak's multiple comparisons test) within a developmental stage. Letters denote significant difference ($p < 0.05$) between developmental stages for *CrLFY1* or *CrLFY2* (Tukey's test). Groups marked with the same letter are not significantly different from each other ($p > 0.05$). Statistical comparisons between developmental stages were considered separately for *CrLFY1* and *CrLFY2*. The use of different letters between *CrLFY1* and *CrLFY2* does not indicate a significant difference.

169 **Spatial expression patterns of CrLFY1 are consistent with a retained ancestral role to facilitate cell
170 divisions during embryogenesis**

171 Functional characterization in *P. patens* previously demonstrated that LFY promotes cell divisions
172 during early sporophyte development (Tanahashi et al., 2005). To determine whether the spatial
173 domains of *CrLFY1* expression are consistent with a similar role in Ceratopteris embryo development,
174 transgenic lines were generated that expressed the reporter gene B-glucuronidase (GUS) driven by 3.9
175 kb of the *CrLFY1* promoter (*CrLFY1_{pro}::GUS*) (**Supplementary File 5**). GUS activity was monitored
176 in individuals from three independent transgenic lines, sampling both before and up to six days after
177 fertilization (**Figure 3A-O**), using wild-type individuals as negative controls (**Figure 3P-T**) and
178 individuals from a transgenic line expressing GUS driven by the constitutive 35S promoter ($35S_{pro}$)
179 (**Supplementary File 5**) as positive controls (**Figure 3U-Y**). Notably, no GUS activity was detected in
180 unfertilized archegonia of *CrLFY1_{pro}::GUS* gametophytes (**Figure 3A, F, K**) but by two days after
181 fertilization (DAF) GUS activity was detected in most cells of the early sporophyte embryo (**Figure 3B,**
182 **G, L**). At 4 DAF, activity was similarly detected in all visible embryo cells, including the embryonic
183 frond, but not in the surrounding gametophytic tissue (the calyptra) (**Figure 3C, H, M**). This embryo-
184 wide pattern of GUS activity became restricted in the final stages of development such that by the end
185 of embryogenesis (6 DAF) GUS activity was predominantly localized in the newly-initiated shoot apex
186 (**Figure 3D, E, I, J, N, O**). Collectively, the GUS activity profiles indicate that *CrLFY1* expression is
187 induced following formation of the zygote, sustained in cells of the embryo that are actively dividing,
188 and then restricted to the shoot apex at embryo maturity. This profile is consistent with the suggestion
189 that *CrLFY1* has retained the LFY role first identified in *P. patens* (Tanahashi et al., 2005), namely to
190 promote the development of a multicellular sporophyte, in part by facilitating the first cell division of
191 the zygote.

192

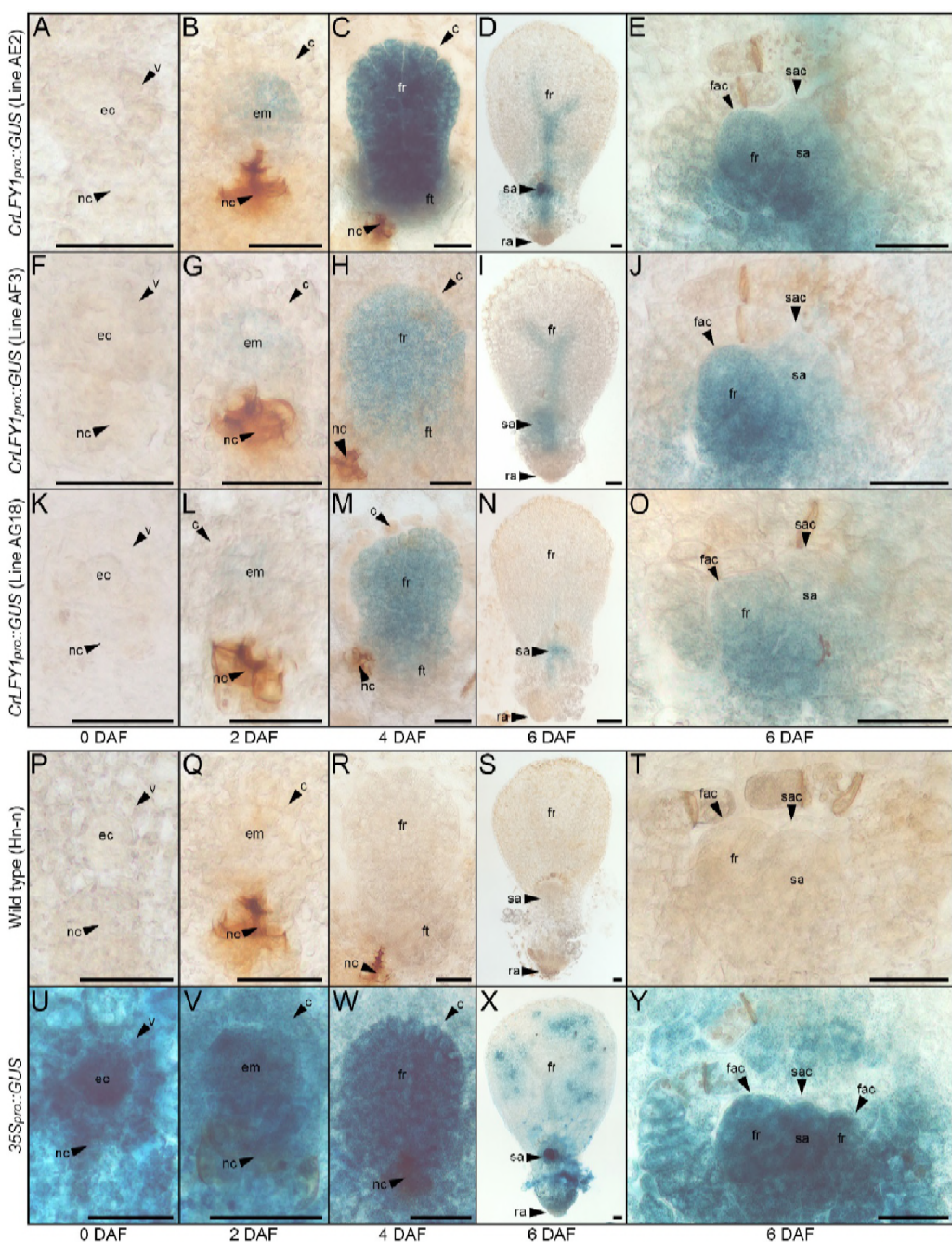


Figure 3. The *CrLFY1* promoter drives reporter gene expression in proliferating tissues of the developing Ceratopteris embryo. A-Y. GUS activity detected as blue staining in developing embryos of three independent *CrLFY1_{pro}::GUS* transgenic reporter lines (A-O), a representative negative wild-type control line (P-T) and a representative positive *35S_{pro}::GUS* control line (U-Y). Tissues are shown prior to fertilization (A, F, K, P, U), or 2 (B, G, L, Q, V), 4 (C, H, M, R, W), and 6 (D, I, N, S, X) days after fertilization (DAF). In *CrLFY1_{pro}::GUS* lines, GUS activity first became visible within the first few divisions of embryo development (but not in surrounding gametophyte tissues) at 2 DAF (B, G, L) and was expressed in cells of the embryo frond as it proliferated (C, H, M). GUS activity was visible in the shoot apex at 6 DAF (D, I, N), with staining in the shoot apical cell (sac), subtending shoot apex tissues and newly-initiated fronds, including the frond apical cell (fac) (E, J, O). No GUS activity was detected in wild-type samples (P-T), whereas the majority of cells in the constitutively expressing *35S_{pro}::GUS* samples stained blue (U-Y). Embryos develop on the surface of the gametophyte thallus when an egg cell (ec) within the archegonium (which comprises a venter (v) and neck canal (nc) to allow sperm entry) are fertilized. After fertilization, the venter forms a jacket of haploid cells known as the calyptra (c) that surrounds the diploid embryo (em). Cell fates in the embryo (embryo frond (fr), embryo foot (ft), root apex (ra) and shoot apex (sa)) are established at the eight-celled stage (Johnson & Renzaglia, 2008), which is around 2 DAF under our growth conditions. Embryogenesis is complete at 6 DAF, after which fronds arise from the shoot apex. Scale bars = 50 µm.

194 **CrLFY1 is expressed in dividing tissues throughout shoot development**

195 Both mosses and ferns form embryos, but moss sporophyte development is determinate post-
196 embryogenesis (Kato and Akiyama, 2005; Kofuji and Hasebe, 2014) whereas fern sporophytes are
197 elaborated from indeterminate shoot apices (Bierhorst, 1977; White and Turner, 1995). *CrLFY1*
198 expression in the shoot apex at the end of embryogenesis (**Figure 3E, J, O**) and elevated transcript
199 levels in shoot apex-containing sporophyte tissues (**Figure 2L**) suggested an additional role for *CrLFY1*
200 relative to that seen in mosses, namely to promote proliferation in the indeterminate shoot apex. To
201 monitor *CrLFY1* expression patterns in post-embryonic sporophytes, GUS activity was assessed in
202 *CrLFY1_{pro}::GUS* lines at two stages of vegetative development (**Figure 4A-O**) and after the transition
203 to reproductive frond formation (**Figure 4-figure supplement 1A-L**). Wild-type individuals were used
204 as negative controls (**Figure 4P-T**; **Figure 4-figure supplement 1M-P**) and *35S_{pro}::GUS* individuals
205 as positive controls (**Figure 4U-Y**; **Figure 4-figure supplement 1Q-T**). In young sporophytes (20
206 DAF), GUS activity was primarily localized in shoot apical tissues and newly-emerging frond primordia
207 (**Figure 4A, F, K**), with very little activity detected in the expanded simple fronds (**Figure 4B, G, L**).
208 In older vegetative sporophytes (60 DAF), which develop complex dissected fronds (**Figure 4C, H, M**),
209 GUS activity was similarly localized in the shoot apex and young frond primordia in two out of the
210 three fully characterized lines (**Figure 4D, I, N**) and in a total of 8 out of 11 lines screened (from seven
211 independent rounds of plant transformation). GUS activity was also detected in developing fronds in
212 regions where the lamina was dividing to generate pinnae and pinnules (**Figure 4E, J, O**). In some
213 individuals GUS activity could be detected in frond tissues almost until maturity (**Figure 4C**). Notably,
214 patterns of *CrLFY1_{pro}::GUS* expression were the same in the apex and complex fronds of shoots before
215 (60 DAF) (**Figure 4C-E, H-J, M-O**) and after (~115 DAF) the reproductive transition (**Figure 4-figure
216 supplement 1A-L**). Consistent with a general role for *CrLFY1* in promoting cell proliferation in the
217 shoot, GUS activity was also detected in shoot apices that initiate *de novo* at the lamina margin between
218 pinnae (**Figure 4Z-AD**). Together these data support the hypothesis that *LFY* function was recruited to
219 regulate cell division processes in the shoot when sporophytes evolved from determinate to
220 indeterminate structures.

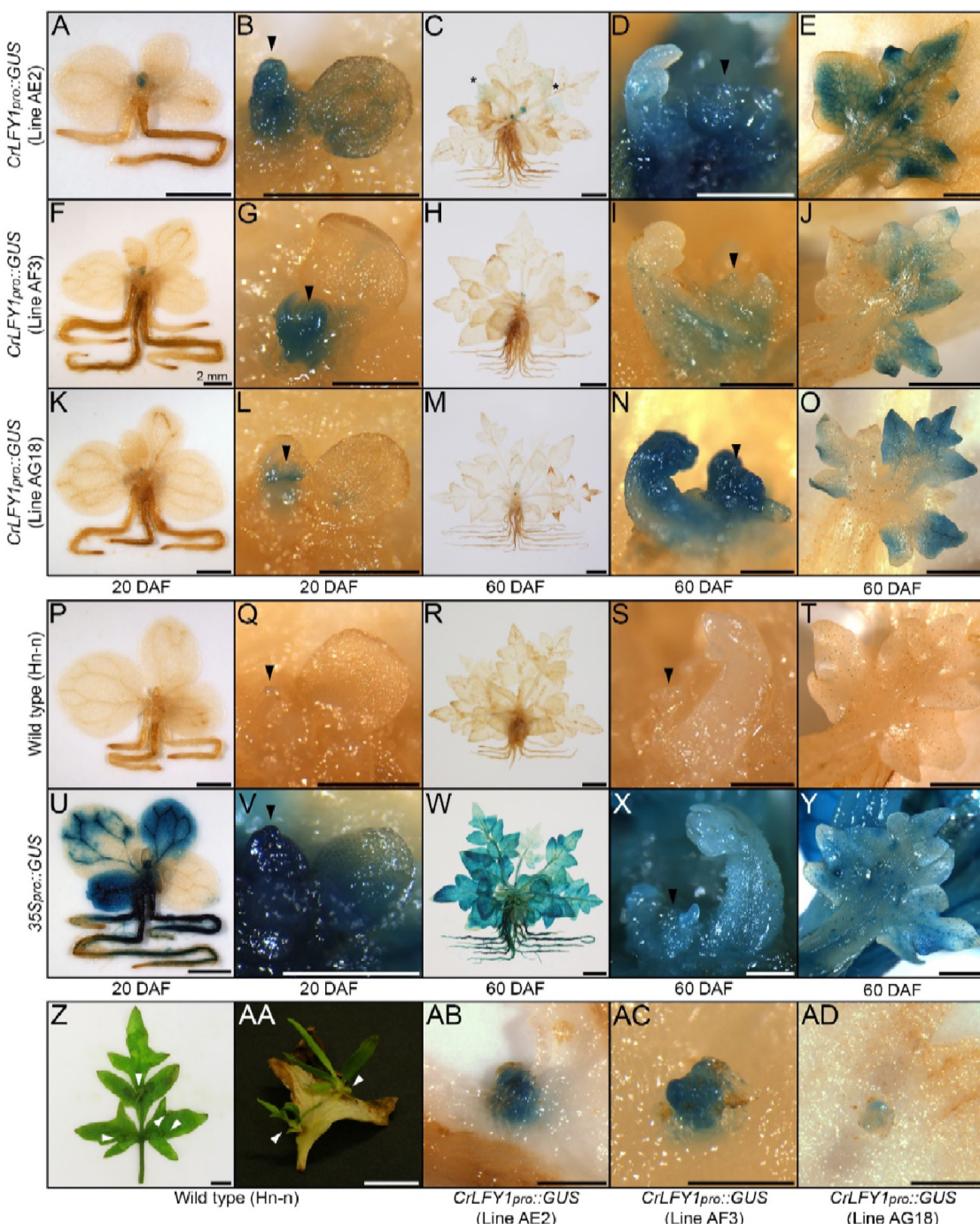


Figure 4. The *CrLFY1* promoter drives reporter gene expression in proliferating shoot tissues of the Ceratopteris sporophyte. A-Y. GUS activity detected as blue staining in post-embryonic sporophytes from three independent *CrLFY1_{pro}::GUS* transgenic reporter lines (A-O), negative wild-type controls (P-T) and positive *35S_{pro}::GUS* controls (U-Y). Sporophytes were examined at 20 DAF (A, B, F, G, K, L, P, Q, U, V) and 60 DAF (C-E, H-J, M-O, R-T, W-Y). GUS staining patterns are shown for whole sporophytes (A, C, F, H, K, M, P, R, U, W), shoot apices (black arrowheads) (B, D, G, I, L, N, Q, S, V, X) and developing fronds (E, J, O, T, Y). In *CrLFY1_{pro}::GUS* sporophytes at 20 DAF (producing simple, spade-like fronds) GUS activity was restricted to the shoot apex (A, F, K) and newly-initiated frond primordia, with very low activity in expanded fronds (B, G, L). In *CrLFY1_{pro}::GUS* sporophytes at 60 DAF (producing complex, highly dissected fronds) GUS activity was similarly restricted to the apex (C, H, M), but persisted for longer during frond development. Activity was initially detected throughout the frond primordium (D, I, N), before becoming restricted to actively proliferating areas of the lamina (E, J, O). Scale bars = 2 mm (A, F, K, P, U), 500 µm (B, D, G, I, L, N, Q, S, V, X) 10 mm (C, H, M, R, W), 1 mm (E, J, O, T, Y). * = GUS staining in maturing frond. GUS staining patterns were the same in leaves formed after the reproductive transition (**Figure 4-figure supplement 1**). Z-AD. Fronds can initiate *de novo* shoots (white arrowheads) from marginal tissue between existing frond pinnae (Z, AA). GUS activity was detected in emerging *de novo* shoot apices on *CrLFY1_{pro}::GUS* fronds (AB-AD). Scale bars = 10 mm (Z, AA), 500 µm (AB-AD).

222 **CrLFY1 regulates activity of the sporophyte shoot apex**

223 To test the functional significance of *CrLFY* expression patterns, transgenic RNAi lines were generated
224 in which one of four RNAi constructs targeted to *CrLFY1*, *CrLFY2* or both were expressed from the
225 maize ubiquitin promoter (*ZmUbi_{pro}*) (**Supplementary File 6**). Phenotypic screening identified 10 lines
226 with similar developmental defects that were associated with reduced *CrLFY* expression (**Table 1**).
227

RNAi transgene	Line	Transformation replicate	Gametophyte phase				Sporophyte phase				
			Spore germination	AC-based growth	Notch meristem-based growth	% Population arrested	Embryo	Shoot apex initiated	Simple frond	Complex frond	% Population arrested
<i>ZmUbi_{pro}::CrLFY1/2-i1</i>	B16	1	+	-	-	99.86	+	+	-	-	<5%
<i>ZmUbi_{pro}::CrLFY1/2-i1</i>	B19	1	+	-	-	50.00	+	+	+	-	<5%
<i>ZmUbi_{pro}::CrLFY1/2-i1</i>	D13	2	+	-	-	99.80	+	+	-	-	<5%
<i>ZmUbi_{pro}::CrLFY1/2-i1</i>	D2	3	+	+	+	0.00	+	+	-	-	<5%
<i>ZmUbi_{pro}::CrLFY1/2-i1</i>	D4	3	+	+	+	0.00	+	+	+	+	<5%
<i>ZmUbi_{pro}::CrLFY1/2-i2</i>	F9	4	+	-	-	0.00	+	+	-	-	<5%
<i>ZmUbi_{pro}::CrLFY1/2-i2</i>	F14	5	-	-	-	100.00	-	-	-	-	-
<i>ZmUbi_{pro}::CrLFY1-i3</i>	E8	6	+	+/-	+/-	100.00	-	-	-	-	-
<i>ZmUbi_{pro}::CrLFY1-i3</i>	G13	7	+	+	+	0.00	+	+	-	-	<5%
<i>ZmUbi_{pro}::CrLFY2-i4</i>	C3	9	+	+	+	0.00	+	+	-	-	<5%

Table 1. Summary of *CrLFY* RNAi transgenic lines and their phenotypic characterization. Transgenic lines exhibited gametophytic developmental arrest and/or sporophyte shoot termination at varying stages of development. ‘+’ indicates that a particular line was phenotypically normal at the developmental stage indicated, ‘-’ indicates that development had arrested at or prior to this stage. In lines marked ‘+/-’ the stage at which developmental defects occurred varied between individuals within the line, and at least some arrested individuals were identified at the stage indicated. The five *ZmUbi_{pro}::CrLFY1/2-i1* lines shown were generated from three rounds of transformation, the pairs of lines B16 and B19 and D2 and D4 potentially arising from the same transformation event. For all other constructs each transgenic line arose from a separate round of transformation and so must represent independent T-DNA insertions.

228

229

230 Wild-type post-embryonic shoot development begins with the production of simple, spade-like fronds
231 from the shoot apex (**Figure 5A**). In eight transgenic lines, sub-populations of sporophytes developed
232 in which early sporophyte development was perturbed, one line (E8) failing to initiate recognizable
233 embryos (**Figure 5B**) and the remainder exhibiting premature shoot apex termination, typically after
234 producing several distorted fronds (**Figure 5C-H**). Sub-populations of phenotypically normal
235 transgenic sporophytes were also identified in some of these lines (**Figure 5I-L**). The two remaining
236 lines exhibited less severe shoot phenotypes, one (B19) undergoing shoot termination only when wild-
237 type sporophytes produced complex fronds (**Figure 5M, N**) and the other (D4a) completing sporophyte

development but reduced in size to approximately 50% of wild-type (**Figure 5O, P**). Despite the predicted sequence specificity of *CrLFY1-i3* and *CrLFY2-i4* (**Supplementary File 6**), quantitative RT-PCR analysis found that all four RNAi constructs led to suppressed transcript levels of both *CrLFY* genes (**Figure 5Q**). The severity of the shoot phenotype was correlated with the level of endogenous *CrLFY* transcripts detected across all lines (**Figure 5Q**), with relative levels of both *CrLFY1* and *CrLFY2* significantly reduced compared to wild-type in all early-terminating sporophytes ($p < 0.0001$ and $p < 0.01$, respectively). Notably, phenotypic differences between the two less-severe lines correlated with differences in *CrLFY1* transcript levels, which were significantly reduced ($p < 0.01$) in late-terminating line B19 but not significantly different from wild-type ($p > 0.05$) in the non-arresting line D4a. *CrLFY2* expression was not significantly different from wild-type ($p > 0.05$) in either the B19 or D4a line, or in the phenotypically normal transgenics. Together these data indicate that wild-type levels of *CrLFY2* are sufficient to compensate for some loss of *CrLFY1*, but at least 10% of wild-type *CrLFY1* activity is required to prevent premature termination of the shoot apex. It can thus be concluded that *CrLFY1* and *CrLFY2* act partially redundantly to maintain indeterminacy of the shoot apex in Ceratopteris, a role not found in the early divergent bryophyte *P. patens*, nor known to be retained in the majority of later diverging flowering plants.

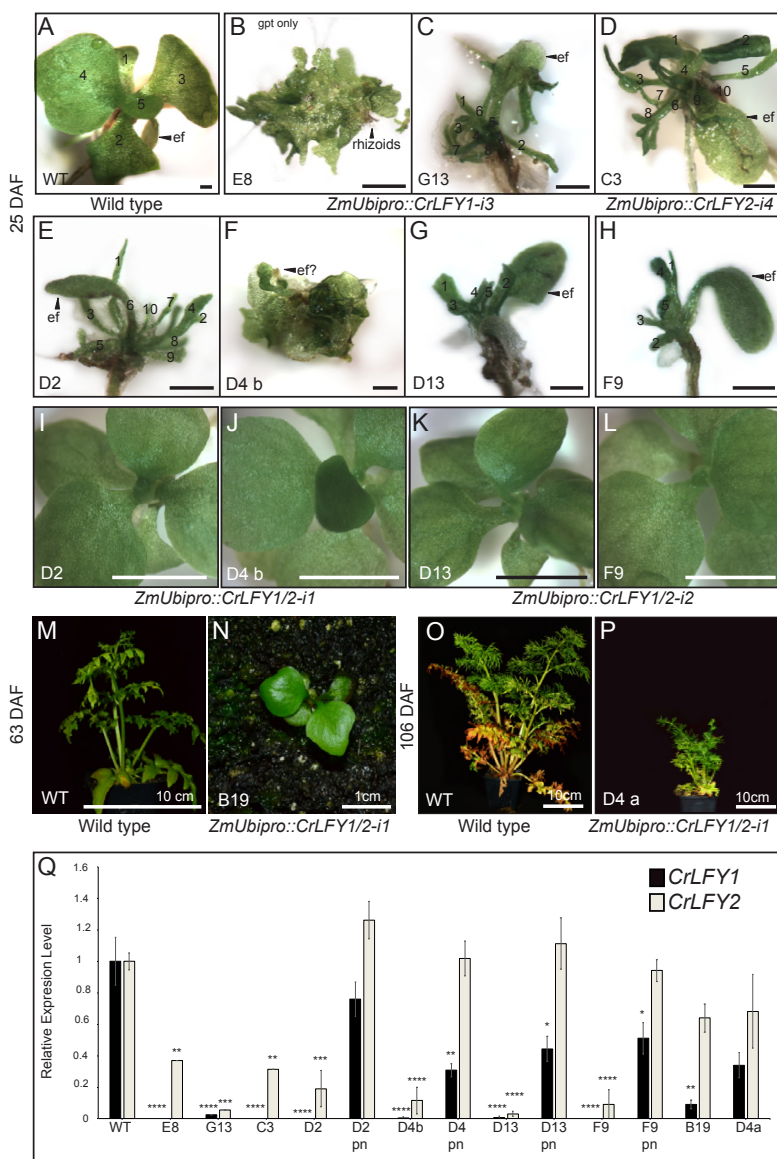


Figure 5. Suppression of *CrLFY* expression causes early termination of the *Ceratopteris* sporophyte shoot apex. A-L. Sporophyte phenotype 25 days after fertilization (DAF) in wild-type (A) and transgenic lines carrying RNAi constructs against *CrLFY1* (*ZmUbi_{pro}::CrLFY1-i3*) (B, C), *CrLFY2* (*ZmUbi_{pro}::CrLFY1-i4*) (D) and both *CrLFY1* and *CrLFY2* (*ZmUbi_{pro}::CrLFY1/2-i1* and *ZmUbi_{pro}::CrLFY1/2-i2*) (E-L). In some lines, both aborted and phenotypically normal sporophytes were identified (compare E & I; F & J; G & K; H & L). The presence of the RNAi transgene in phenotypically normal sporophytes was validated by genotyping (Supplementary File 6). Scale bars = 100 µm (A-H), 5mm (I-L). **M-P.** Sporophyte phenotype of wild-type (M, O) and two *ZmUbi_{pro}::CrLFY1/2-i1* lines (N, P) at 63 (M, N) and 106 (O, P) DAF. Scale bars = 1cm (O), 10cm (M, O, P). **Q.** qRT-PCR analysis of *CrLFY1* and *CrLFY2* transcript levels (normalized against the averaged expression of housekeeping genes *CrACTIN1* and *CrTBP*) in the sporophytes of the RNAi lines shown in (A-P). Transcript levels are depicted relative to wild type. n = 3, error bars = standard error of the mean (SEM). *CrLFY1* and *CrLFY2* expression levels were significantly reduced compared to wild type ($\leq 1\%$ and 3-19%, respectively) in all transgenic lines where sporophyte shoots undergo early termination (A-H), but in phenotypically normal (pn) sporophytes segregating in the same lines (I-L), only *CrLFY1* transcript levels were reduced (D4b, p < 0.01; D13, F9, p < 0.05). *CrLFY2* transcript levels were not significantly different from wild-type in the phenotypically normal sporophytes at 25 DAF (I-L) or in the sporophytes that survived to 63 (N) or 106 (P) DAF. *CrLFY1* levels were significantly reduced (~10%) in line B19 where shoot termination occurred ~63 DAF (N) but were not significantly different from wild type in line D4a where shoot development did not terminate prematurely (P). Asterisks denote level of P were significant difference (*, p < 0.05; **, p < 0.01, ***, p < 0.001; ****, p < 0.0001) from wild type.

255 **CrLFY promotes apical cell divisions in the gametophyte**

256 In six of the RNAi lines that exhibited sporophyte developmental defects, it was notable that 50%-99%
257 of gametophytes arrested development prior to the sporophyte phase of the lifecycle (**Table 1**). This
258 observation suggested that LFY plays a role in Ceratopteris gametophyte development, a function not
259 previously recognized in either bryophytes or angiosperms. During wild-type development, the
260 Ceratopteris gametophyte germinates from a single-celled haploid spore, establishing a single apical
261 cell (AC) within the first few cell divisions (**Figure 6A**). Divisions of the AC go on to form a two-
262 dimensional photosynthetic thallus in both the hermaphrodite (**Figure 6B**) and male sexes (**Figure 6C**).
263 In contrast, the gametophytes from six RNAi lines (carrying either *ZmUbi_{pro}::CrLFY1-i3*,
264 *ZmUbi_{pro}::CrLFY1/2-i1* or *ZmUbi_{pro}::CrLFY1/2-i2*) exhibited developmental arrest (**Figure 6D-J**),
265 which in five lines clearly related to a failure of AC activity. The point at which AC arrest occurred
266 varied, in the most severe line occurring prior to or during AC specification (**Figure 6D**) and in others
267 during AC-driven thallus proliferation (**Figure 6E-I**). Failure of AC activity was observed in both
268 hermaphrodites (**Figure 6E**) and males (**Figure 6H, I**). The phenotypically least severe line exhibited
269 hermaphrodite developmental arrest only after AC activity had been replaced by the notch meristem
270 (**Figure 6J**). A role for *CrLFY* in maintenance of gametophyte AC activity was supported by the
271 detection of *CrLFY* transcripts in the AC and immediate daughter cells of wild-type gametophytes
272 (**Figure 6K-N**). By contrast *CrLFY* transcripts were not detected in arrested *ZmUbi_{pro}::CrLFY1/2-i1*
273 lines (**Figure 6O-R**) despite confirmed presence of the transgene (**Figure 6- figure supplement 1**).
274 Although the observed phenotypes could not be ascribed to a specific gene copy, these data support a
275 role for *CrLFY* in AC maintenance during gametophyte development, and thus invoke a role for LFY
276 in the regulation of apical activity in both the sporophyte and gametophyte phases of vascular plant
277 development.

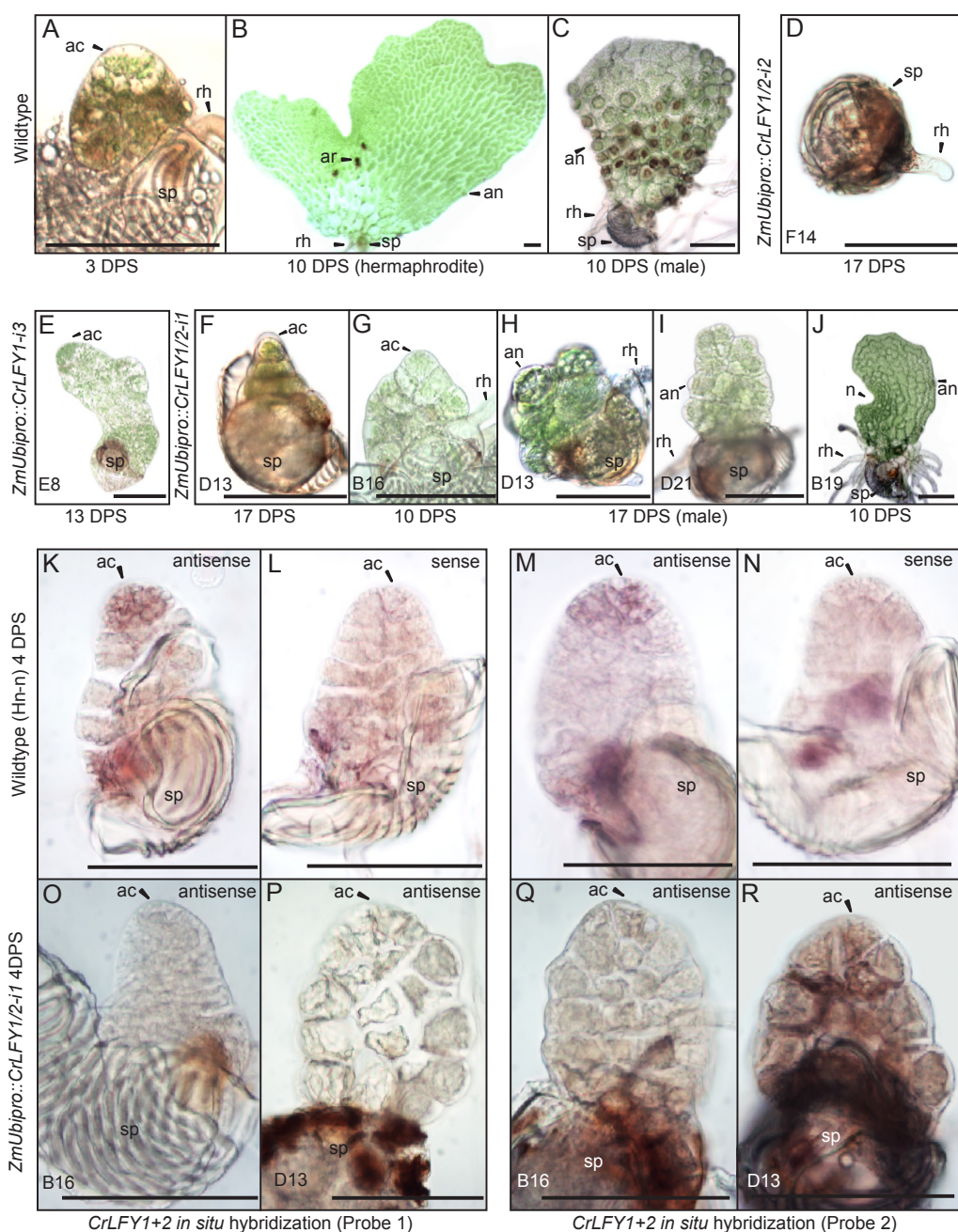


Figure 6. Suppression of *CrLFY* expression causes early termination of the Ceratopteris gametophyte apical cell. **A-C.** The wild-type Ceratopteris gametophyte establishes a triangular apical cell (ac) shortly after spore (sp) germination (**A**). Divisions of the apical cell establish a photosynthetic thallus in both hermaphrodite and male gametophytes. At 10 days post spore sowing (DPS) both gametophyte sexes are approaching maturity, with the hermaphrodite (**B**) having formed a chordate shape from divisions at a lateral notch meristem (n) and having produced egg-containing archegonia (ar), sperm-containing antheridia (an), and rhizoids (rh). The male (**C**) has a more uniform shape with antheridia across the surface. **D-J.** When screened at 10-17 DPS, gametophytes from multiple RNAi lines (as indicated) exhibited developmental arrest, mostly associated with a failure of apical cell activity. Arrest occurred at various stages of development from failure to specify an apical cell, resulting in only a rhizoid being produced and no thallus (**D**) through subsequent thallus proliferation (**E-I**). Gametophyte development in one line progressed to initiation of the notch meristem but overall thallus size was severely reduced compared to wild-type (**J**). **K-R.** *In situ* hybridization with antisense probes detected *CrLFY* transcripts in the apical cell and immediate daughter cells of wild-type gametophytes at 4 DPS (**K, M**). No corresponding signal was detected in controls hybridized with sense probes (**L, N**). In the arrested gametophytes of two *ZmUbi_{pro}::CrLFY1/2-i1* lines *CrLFY* transcripts could not be detected (**O-R**), and transgene presence was confirmed (**Figure 6-figure supplement 1**). Scale bars = 100 µm.

279 **DISCUSSION**

280 The results reported here reveal a role for LFY in the maintenance of apical cell activity throughout
281 gametophyte and sporophyte shoot development in *Ceratopteris*. During sporophyte development, qRT-
282 PCR and transgenic reporter lines demonstrated that *CrLFY1* is preferentially expressed in the shoot
283 apex (whether formed during embryogenesis or *de novo* on fronds, and both before and after the
284 reproductive transition); in emerging lateral organ (frond) primordia; and in pinnae and pinnules as they
285 form on dissected fronds (**Figures 2-4**). Notably, active cell division is the main feature in all of these
286 contexts. *CrLFY2* transcript levels were more uniform throughout sporophyte shoot development, in
287 both dividing tissues and expanded fronds (**Figure 2**), and expression has previously been reported in
288 roots (Himi et al., 2001). Simultaneous suppression of *CrLFY1* and *CrLFY2* activity by RNAi resulted
289 in developmental arrest of both gametophyte and sporophyte shoot apices, with any fronds produced
290 before termination of the sporophyte apex exhibiting abnormal morphologies (**Figures 5, 6**). The
291 severity of phenotypic perturbations in sporophytes of transgenic lines correlated with combined
292 *CrLFY1* and *CrLFY2* transcript levels, with wild-type levels of *CrLFY2* able to fully compensate for up
293 to a 70% reduction in *CrLFY1* levels (**Figure 5**). The duplicate *CrLFY* genes therefore act at least
294 partially redundantly during shoot development in *Ceratopteris*.

295

296 A function for LFY in gametophyte development has not previously been reported in any land plant
297 species. In the moss *P. patens*, *PpLFY1* and *PpLFY2* are expressed in both the main and lateral apices
298 of gametophytic leafy shoots but double loss of function mutants develop normally; indicating that LFY
299 is not necessary for maintenance of apical cell activity in the gametophyte (Tanahashi et al., 2005). By
300 contrast, loss of *CrLFY* expression from the gametophyte shoot apex results in loss of apical cell activity
301 during thallus formation in *Ceratopteris* (**Figure 6**). The different DNA binding site preferences (and
302 hence downstream target sequences) of *PpLFY* and *CrLFY* (Sayou et al., 2014) may be sufficient to
303 explain the functional distinction in moss and fern gametophytes, but the conserved expression pattern
304 is intriguing given that there should be no pressure to retain that pattern in *P. patens* in the absence of
305 functional necessity. The thalloid gametophytes of the two other extant bryophyte lineages (liverworts

306 and hornworts) resemble the fern gametophyte more closely than mosses (Ligrone et al., 2012), but
307 LFY function in these contexts is not yet known. Overall the data are consistent with the hypothesis that
308 in the last common ancestor of ferns and angiosperms, LFY functioned to promote cell proliferation in
309 the thalloid gametophyte, a role that has been lost in angiosperms where gametophytes have no apical
310 cell and are instead just few-celled determinate structures.

311
312 The range of reported roles for LFY in sporophyte development can be rationalized by invoking three
313 sequential changes in gene function during land plant evolution (**Figure 7**). First, the ancestral LFY
314 function to promote early cell divisions in the embryo was retained as bryophytes and vascular plants
315 diverged, leading to conserved roles in *P. patens* (Tanahashi et al., 2005) and Ceratopteris (**Figure 3**).
316 Second, within the vascular plants (preceding divergence of the ferns) this proliferative role expanded
317 to maintain apical cell activity, and hence to enable indeterminate shoot growth. This is evidenced by
318 *CrLFY* activity at the tips of shoots, fronds and pinnae (**Figures 3-5**), all of which develop from one or
319 more apical cells (Hill, 2001; Hou and Hill, 2004). Whether fern fronds are homologous to shoots or to
320 leaves in angiosperms is an area of debate (Tomescu, 2009; Vasco et al., 2013; Harrison and Morris,
321 2018), but there are angiosperm examples of LFY function in the vegetative SAM (Ahearn et al., 2001;
322 Zhao et al., 2017), axillary meristems (Kanrar et al., 2008; Rao et al., 2008; Chahtane et al., 2013) and
323 in actively dividing regions of compound leaves (Hofer et al., 1997; Molinero-Rosales et al., 1999;
324 Champagne et al., 2007; Wang et al., 2008) indicating that a proliferative role in vegetative tissues has
325 been retained in at least some angiosperm species. Consistent with the suggestion that the angiosperm
326 floral meristem represents a modified vegetative meristem (Theissen et al., 2016), the third stage of LFY
327 evolution would have been co-option and adaptation of this proliferation-promoting network into floral
328 meristems, with subsequent restriction to just the flowering role in many species. This is consistent with
329 multiple observations of *LFY* expression in both vegetative and reproductive shoots (developing cones)
330 in gymnosperms (Mellerowicz et al.; Mouradov et al., 1998; Shindo et al., 2001; Carlsbecker et al.,
331 2004; Vázquez-Lobo et al., 2007; Carlsbecker et al., 2013; Moyroud et al., 2017) and suggests that pre-
332 existing *LFY*-dependent vegetative gene networks might have been co-opted during the origin of

333 specialized sporophyte reproductive axes in ancestral seed plants, prior to the divergence of
 334 angiosperms.

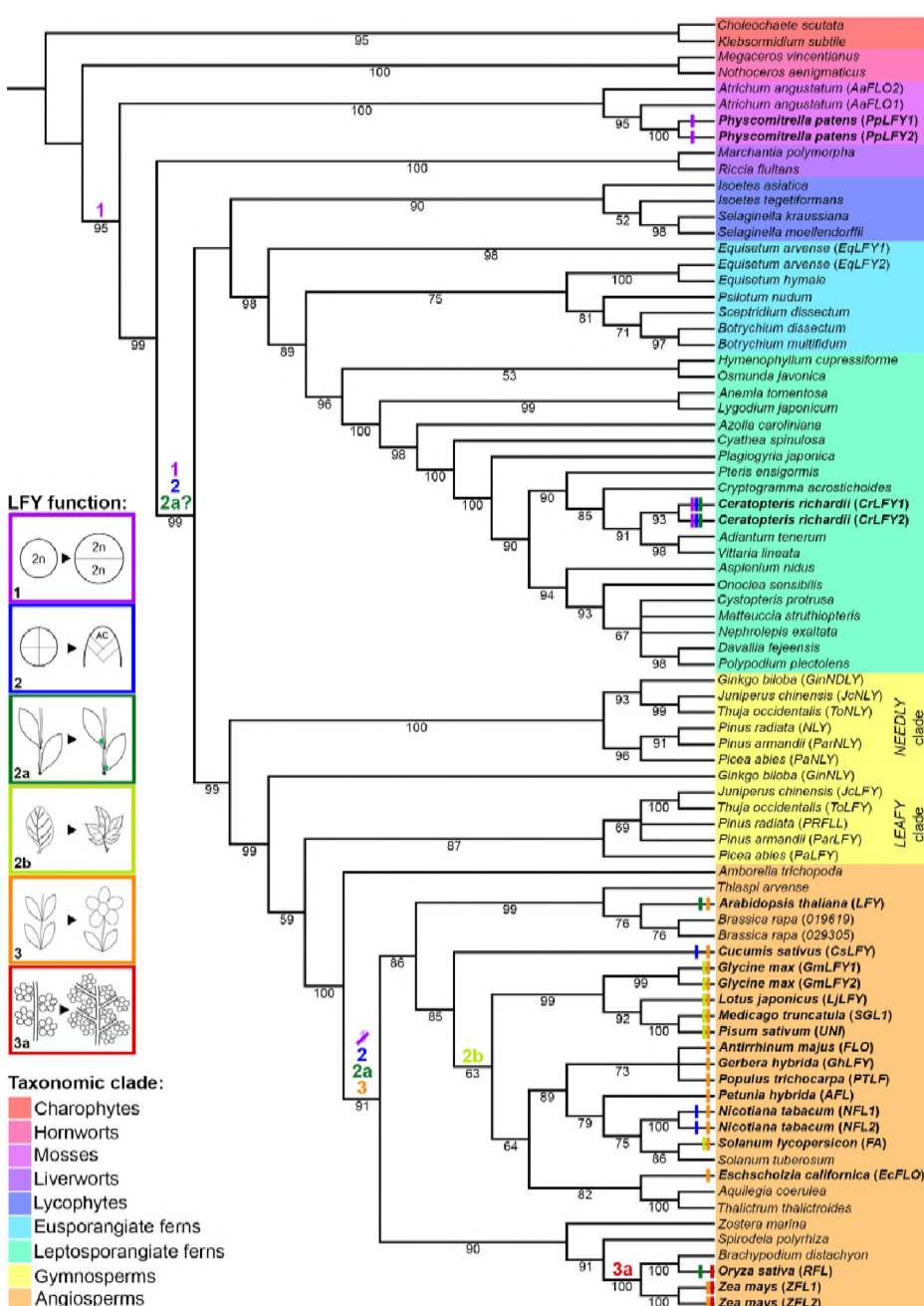


Figure 7. Evolutionary trajectory of LFY function. The phylogeny was reconstructed from selected LFY protein sequences representing all extant embryophyte lineages (as highlighted) and the algal sister-group. Coloured bars at the terminal branches represent different developmental functions of LFY determined from functional analysis in those species (see **Supplementary File 8** for references). Coloured numbers indicate the putative points of origin of different functions inferred from available data points across the tree. **1**, cell division within the sporophyte zygote; **2**, maintenance of indeterminate cell fate in vegetative shoots through proliferation of one or more apical cells (AC); **2a**, maintenance of indeterminate cell fate in vegetative lateral/axillary apices; **2b**, maintenance of indeterminate cell fate in the margins of developing lateral organs (compound leaves); **3**, specification of floral meristem identity (determinate shoot development producing modified lateral organs) and shoot transition to the reproductive phase; **3a**, maintenance of indeterminate cell fate in inflorescence lateral/branch meristems (in place of floral meristem fate).

336 The proposed evolutionary trajectory for LFY function bears some resemblance to that seen for KNOX
337 protein function. Class I *KNOX* genes are key regulators of indeterminacy in the vegetative shoot apical
338 meristem of angiosperms (Gaillochet et al., 2015), and are required for compound leaf formation in both
339 tomato and *Cardamine hirsuta* (Bar and Ori, 2015). In ferns, *KNOX* gene expression is observed both
340 in the shoot apex and developing fronds (Sano et al., 2005; Ambrose and Vasco, 2016), and in *P. patens*
341 the genes regulate cell division patterns in the determinate sporophyte (Sakakibara et al., 2008). It can
342 thus be speculated that *LFY* and *KNOX* had overlapping functions in the sporophyte of the last common
343 ancestor of land plants, but by the divergence of ancestral angiosperms from gymnosperms, *KNOX*
344 genes had come to dominate in vegetative meristems whereas *LFY* became increasingly specialized for
345 floral meristem function. Unlike *LFY*, however, there is not yet any evidence for *KNOX* function in the
346 gametophyte of any land plant lineage, and thus if a pathway for regulating stem cell activity was co-
347 opted from the gametophyte into the sporophyte, it was the *LFY* pathway.
348

349 MATERIALS AND METHODS

350 *Plant materials and growth conditions*

351 All experimental work was conducted using *Ceratopteris richardii* strain Hn-n (Hickok et al., 1995).
352 Plant growth conditions for Ceratopteris transformation and DNA gel blot analysis of transgenic lines
353 were as previously described (Plackett et al., 2015).
354

355 *Phylogenetic analysis*

356 A dataset of 99 aligned LFY protein sequences from a broad range of streptophytes was first retrieved
357 from Sayou et al., (2014). The dataset was pruned and then supplemented with further sequences
358 (**Supplementary File 1**) to enable trees to be inferred that would (i) provide a more balanced
359 distribution across the major plant groups and (ii) infer fern relationships. Only a subset of available
360 angiosperm sequences was retained (keeping both monocot and dicot representatives) but protein
361 sequences from other angiosperm species where function has been defined through loss-of-function
362 analyses were added from NCBI – *Antirrhinum majus* FLO AAA62574.1 (Coen et al. 1990), *Pisum*

363 *sativum* UNI AAC49782.1 (Hofer *et al.* 1997), *Cucumis sativus* CsLFY XP_004138016.1 (Zhao *et al.*
364 2017), *Medicago truncatula* SGL1 AY928184 (Wang *et al.* 2008), *Petunia hybrida* ALF AAC49912.1
365 (Souer *et al.* 1998), *Nicotiana tabacum* NFL1 AAC48985.1 and NFL2 AAC48986.1 (Kelly *et al.* 1995),
366 *Eschscholzia californica* EcFLO AAO49794.1 (Busch & Gleissberg 2003), *Gerbera hybrida* cv.
367 ‘Terraregina’ GhLFY ANS10152.1 (Zhao *et al.* 2016), *Lotus japonicus* LjLFY AAX13294.1 (Dong *et*
368 *al.* 2005) and *Populus trichocarpa* PTLF AAB51533.1 (Rottmann *et al.* 2000). To provide better
369 resolution within and between angiosperm clades, sequences from *Spirodela polyrhiza* (32G0007500),
370 *Zostera marina* (27g00160.1), *Aquilegia coerulea* (5G327800.1) and *Solanum tuberosum*
371 (PGSC0003DMT400036749) were added from Phytozome v12.1
372 (<https://phytozome.jgi.doe.gov/pz/portal.html>). Genome sequence from the early-diverging Eudicot
373 *Thalictrum thalictroides* was searched by TBLASTX (Altschul *et al.*, 1990)
374 (https://blast.ncbi.nlm.nih.gov/Blast.cgi?PROGRAM=tblastx&PAGE_TYPE=BlastSearch&BLAST_SPEC=&LINK_LOC=blasttab) with nucleotide sequence from the Arabidopsis *LFY* gene. A gene
375 model was derived from sequence in two contigs (108877 & 116935) using Genewise
376 (<https://www.ebi.ac.uk/Tools/psa/genewise/>). Gymnosperm sequences were retained from *Ginkgo*
377 *biloba* and from a subset of conifers included in Sayou *et al.*, (2014), whilst sequences from conifers
378 where *in situ* hybridization patterns have been reported were added from NCBI – *Pinus radiata* PRFLL
379 AAB51587.1 and NLY AAB68601.1 (Mellerowicz *et al.*; Mouradov *et al.*, 1998) and *Picea abies*
380 PaLFY AAV49504.1 and PaNLY AAV49503.1 (Carlsbecker *et al.*, 2004). Fern sequences were
381 retained except *Angiopteris spp* sequences which consistently disrupted the topology of the tree by
382 grouping with gymnosperms. To better resolve relationships within the ferns, additional sequences
383 were identified in both NCBI and 1KP (Matasci *et al.*, 2014) databases. The protein sequence from
384 *Matteuccia struthiopteris* AAF77608.1 MatstFLO (Himi *et al.*, 2001) was retrieved from NCBI. Further
385 sequences from horsetails (2), plus eusporangiatae (1) and leptosporangiatae (53) ferns were retrieved
386 from the 1KP database (<https://db.cngb.org/blast/>) using BLASTP and the MatstFLO sequence as a
387 query. Lycophyte and bryophyte sequences were all retained, but the liverwort *Marchantia polymorpha*
388 predicted ORF sequence was updated from Phytozome v12.1 (Mpo0113s0034.1.p), the hornwort

390 *Nothoceros* genome scaffold was replaced with a translated full length cDNA sequence (AHJ90704.1)
391 from NCBI and two additional lycophyte sequences were added from the 1KP dataset (*Isoetes*
392 *tegetiformans* scaffold 2013584 and *Selaginella kraussiana* scaffold 2008343). All of the charophyte
393 scaffold sequences were substituted with *Coleochaete scutata* (AHJ90705.1) and *Klebsormidium*
394 *subtile* (AHJ90707.1) translated full-length cDNAs from NCBI.

395

396 The new/replacement sequences were trimmed and amino acids aligned to the existing alignment from
397 Sayou et al. (2014) using CLUSTALW (**Supplementary Files 2 and 3**). The best-fitting model
398 parameters (JTT+I+G4) were estimated and consensus phylogenetic trees were run using Maximum
399 Likelihood from 1000 bootstrap replicates, using IQTREE (Nguyen et al., 2015). Two trees were
400 inferred. The first contained only a subset of fern and allied sequences to achieve a more balanced
401 distribution across the major plant groups (81 sequences in total) (**Figure 7**), whereas the second used
402 the entire dataset (120 sequences ~50% of which are fern and allied sequences – **Figure 1-figure**
403 **supplement 1**). The data were imported into iTOL (Letunic and Bork, 2016) to generate the pictorial
404 representations. All branches with less than 50% bootstrap support were collapsed. Relationships within
405 the ferns (**Figure 1**) were represented by pruning the lycophyte and fern sequences (68 in total) from
406 the tree containing all available fern sequences (**Figure 1-figure supplement 1**).

407

408 *CrLFY locus characterization and DNA gel blot analysis*

409 Because no reference genome has yet been established for Ceratopteris (or any fern), *CrLFY* copy
410 number was quantified by DNA gel blot analysis. Ceratopteris genomic DNA was hybridized using
411 both the highly conserved LFY DNA-binding domain diagnostic of the *LFY* gene family (Maizel, 2005)
412 and also gene copy-specific sequences (**Figure 1-figure supplement 2**). CrLFY1 and CrLFY2 share
413 85% amino acid similarity, compared to 65% and 44% similarity of each to AtLFY. DNA gel blotting
414 and hybridization was performed as described previously (Plackett et al., 2014). The results supported
415 the presence of only two copies of *LFY* within the Ceratopteris genome. All primers used in probe
416 preparation are supplied in **Supplementary File 7**.

417 Genomic sequences for *CrLFY1* and *CrLFY2* ORFs were amplified by PCR from wild-type genomic
418 DNA using primers designed against published transcript sequences (Himi et al., 2001). ORFs of
419 1551bp and 2108bp were obtained, respectively (**Figure 1-figure supplement 2**). Exon structure was
420 determined by comparison between genomic and transcript sequences. The native promoter region of
421 *CrLFY1* was amplified from genomic template by sequential rounds of inverse PCR with initial primer
422 pairs designed against published *CrLFY1* 5'UTR sequence and additional primers subsequently
423 designed against additional contiguous sequence that was retrieved. A 3.9 kb contiguous promoter
424 fragment was isolated for *CrLFY1* containing the entire published 5'UTR and 1.9 kb of additional
425 upstream sequence (**Figure 1-figure supplement 2, Supplementary File 7**).

426

427 *qPCR analysis of gene expression*

428 RNA was extracted from Ceratopteris tissues using the Spectrum Total Plant RNA kit (Sigma-Aldrich,
429 St. Louis, MO) and 480 ng were used as template in iScript cDNA synthesis (Bio-Rad). *CrLFY1* and
430 *CrLFY2* locus-specific qPCR primers (**Supplementary File 7**) were designed spanning intron 1.
431 Amplification specificity of primers was validated via PCR followed by sequencing. qPCR of three
432 biological replicates and three technical replicates each was performed in a Bio-Rad CFX Connect with
433 iTaq Universal SYBR Green Supermix (Bio-Rad, Hercules, CA). Primer amplification efficiency was
434 checked with a cDNA serial dilution. Efficiency was determined using the slope of the linear regression
435 line as calculated by Bio-Rad CFX Connect software. Primer specificity was tested via melting curve
436 analysis, resulting in a single peak per primer set. *CrLFY* expression was calculated using the $2^{-\Delta\Delta Ct}$
437 method (Livak and Schmittgen, 2001) and normalized against the geometric mean of the expression of
438 two endogenous housekeeping genes (Hellemans et al., 2007), *CrACTIN1* and *CrTATA-BINDING*
439 *PROTEIN (TBP)* (Ganger et al., 2014). The standard deviation of the Ct values of each housekeeping
440 gene was calculated to ensure minimal variation (<3%) in gene expression in wild-type versus
441 transgenic lines.

442

443 Relative expression values of *CrLFY* from qPCR were compared by two-way analysis of variance
444 (ANOVA) for developmental stages or transgenic lines, followed by Sidak's or Tukey's multiple
445 comparisons in Prism v. 7.0 (GraphPad Software, Inc., La Jolla, CA). The significance threshold (p)
446 was set at 0.05.

447

448 *Generation of GUS reporter constructs*

449 The *CrLFY1_{pro}::GUS* reporter construct (**Supplementary File 5**) was created by cloning the *CrLFY1*
450 promoter (**Supplementary File 7**) into pART7 as a *NotI-XbaI* restriction fragment, replacing the
451 existing *35S* promoter. A β-Glucuronidase (GUS) coding sequence was cloned downstream of *pCrLFY1*
452 as an *XbaI-XbaI* fragment. The same GUS *XbaI-XbaI* fragment was also cloned into pART7 to create a
453 *35S_{pro}::GUS* positive control. The resulting *CrLFY1_{pro}::GUS::ocs* and *35S_{pro}::GUS::ocs* cassettes were
454 each cloned as *NotI-NotI* fragments into the pART27-based binary transformation vector pBOMBER
455 carrying a hygromycin resistance marker previously optimized for Ceratopteris transformation (Plackett
456 et al., 2015).

457

458 *Generation of RNAi constructs*

459 RNAi constructs were designed and constructed using the pANDA RNAi expression system (Miki and
460 Shimamoto, 2004). Four RNAi fragments were designed, two targeting a conserved region of the
461 *CrLFY1* and *CrLFY2* coding sequence (77% nucleotide identity) using sequences from either *CrLFY1*
462 (*CrLFY1/2-i1*) or *CrLFY2* (*CrLFY1/2-i2*), and two targeting gene-specific sequence within the 3'UTR
463 of *CrLFY1* (*CrLFY1-i3*) or *CrLFY2* (*CrLFY2-i4*) (**Supplementary File 6**). Target fragments were
464 amplified from cDNA and cloned into Gateway-compatible entry vector pDONR207. Each sequence
465 was then recombined into the pANDA expression vector via Gateway LR cloning (Invitrogen, Carlsbad,
466 CA).

467

468

469

470 *Generation of transgenic lines*

471 Transformation of all transgenes into wild-type Hn-n Ceratopteris callus was performed as previously
472 described (Plackett et al., 2015). Transgenic lines were assessed in the T₁ generation for T-DNA copy
473 number by DNA gel blot analysis and the presence of full-length T-DNA insertions was confirmed
474 through genotyping PCR (**Supplementary Files 5 and 6**).

475

476 *GUS staining*

477 GUS activity analysis in *CrLFY1_{pro}::GUS* transgenic lines was conducted in the T₁ generation. GUS
478 staining was conducted as described previously (Plackett et al., 2014). Optimum staining conditions
479 (1mg/ml X-GlcA, 5uM potassium ferricyanide) were determined empirically. Tissue was cleared with
480 sequential incubations in 70% ethanol until no further decolorization occurred.

481

482 *Phenotypic characterization*

483 Phenotypic characterization of RNAi transgenic lines was conducted in the T₂ or T₃ generation. Isogenic
484 lines were obtained by isolating hermaphrodite gametophytes in individual wells at approximately 7
485 DPS (or when the notch became visible, whichever came first) and flooding them once they had
486 developed mature gametangia (at approximately 9 DPS). All transgenic lines were grown alongside
487 wild-type controls and phenotypes observed and recorded daily. Gametophytes exhibiting altered
488 phenotypes were imaged at approximately 10 DPS with a Nikon Microphot-FX microscope.
489 Sporophytes with abnormal phenotypes were imaged with a dissecting microscope.

490

491 *In situ hybridization*

492 Antisense and sense RNA probes for *CrLFY1* and *CrLFY2* were amplified and cloned into pCR 4-TOPO
493 (Invitrogen) and DIG-labelled according to the manufacturer's instructions (Roche, Indianapolis, IN).
494 Probes were designed to include the 5'UTR and ORF (*CrLFY1* 521bp 5'UTR and 1113bp ORF; *CrLFY2*
495 301bp 5'UTR and 1185bp ORF) (**Supplementary File 7**). Tissue was fixed in FAA (3.7%
496 formaldehyde, 5% acetic acid; 50 % ethanol) for 1-4 hours and then stored in 70% ethanol. Whole

497 mount *in situ* hybridization was carried out based on Hejátko et al. (2006), with the following
498 modifications: hybridization and wash steps were carried out in 24-well plates with custom-made
499 transfer baskets (0.5 mL microcentrifuge tubes and 30 µm nylon mesh, Small Parts Inc., Logansport,
500 IN). Permeabilization and post-fixation steps were omitted depending on tissue type, to avoid damaging
501 fragile gametophytes, Acetic Anhydride (Sigma-Aldrich) and 0.5% Blocking Reagent (Roche) washing
502 steps were added to decrease background staining, and tissue was hybridized at 45°C. Photos were
503 taken under bright-field with a Q-imaging Micro-published 3.3 RTV camera mounted on a Nikon
504 Microphot-FX microscope. Images were minimally processed for brightness and contrast in Photoshop
505 (CS4).

506

507 REFERENCES

- 508 **Ahearn KP, Johnson HA, Weigel D, Wagner DR** (2001) NFL1, a *Nicotiana tabacum* LEAFY-like
509 gene, controls meristem initiation and floral structure. *Plant Cell Physiol* **42**: 1130–1139
- 510 **Altschul SF, Gish W, Miller W, Myers EW, Lipman DJ** (1990) Basic local alignment search tool. *J
511 Mol Biol* **215**: 403–410
- 512 **Ambrose BA, Vasco A** (2016) Bringing the multicellular fern meristem into focus. *New Phytol* **210**:
513 790–793
- 514 **Bar M, Ori N** (2015) Compound leaf development in model plant species. *Curr Opin Plant Biol* **23**:
515 61–69
- 516 **Becker A, Gleissberg S, Smyth DR** (2005) Floral and Vegetative Morphogenesis in California Poppy
517 (*Eschscholzia californica* Cham.). *Int J Plant Sci* **166**: 537–555
- 518 **Bierhorst DW** (1977) On the stem apex, leaf initiation and early leaf ontogeny in filicalean ferns. *Am
519 J Bot* **64**: 125–152
- 520 **Blazquez MA, Soowal LN, Lee I, Weigel D** (1997) Leafy expression and flower initiation in
521 *Arabidopsis*. *Development* **124**: 3835–3844
- 522 **Bomblies K, Wang RL, Ambrose BA, Schmidt RJ, Meeley RB, Doebley J** (2003) Duplicate
523 FLORICAULA/LEAFY homologs *zfl1* and *zfl2* control inflorescence architecture and flower

- 524 patterning in maize. *Development* **130**: 2385–2395
- 525 **Bowman JL, Sakakibara K, Furumizu C, Dierschke T** (2016) Evolution in the Cycles of Life. *Annu*
526 *Rev Genet* **50**: 133–154
- 527 **Bradley D, Ratcliffe O, Vincent C, Carpenter R, Coen ES** (1997) Inflorescence Commitment and
528 Architecture in *Arabidopsis*. *Science* (80-) **275**: 80-83
- 529 **Bradley D, Vincent C, Carpenter R, Coen E** (1996) Pathways for inflorescence and floral induction
530 in *Antirrhinum*. *Development* **122**: 1535 LP-1544
- 531 **Busch A, Gleissberg S** (2003) *EcFLO*, a *FLORICAULA*-like gene from *Eschscholzia californica* is
532 expressed during organogenesis at the vegetative shoot apex. *Planta* **217**: 841–848
- 533 **Carlsbecker A, Sundström Jens, Englund M, Uddenberg D, Izquierdo L, Kvarnheden A,**
534 **Vergara-Silva F, Peter E** (2013) Molecular control of normal and acrocona mutant seed cone
535 development in Norway spruce (*Picea abies*) and the evolution of conifer ovule-bearing organs.
536 *New Phytol* **200**: 261–275
- 537 **Carlsbecker A, Tandre K, Johanson U, Englund M, Engström P** (2004) The MADS-box gene
538 DAL1 is a potential mediator of the juvenile-to-adult transition in Norway spruce (*Picea abies*).
539 *Plant J* **40**: 546–557
- 540 **Carpenter R, Coen E** (1990) Floral homeotic mutations produced by transposon mutagenesis in
541 *Antirrhinum majus*. *Genes Dev* **4**: 1483–1493
- 542 **Chahtane H, Vachon G, Masson M, Thévenon E, Périgon S, Mihajlovic N, Kalinina A, Michard**
543 **R, Moyroud E, Monniaux M, et al** (2013) A variant of LEAFY reveals its capacity to stimulate
544 meristem development by inducing RAX1. *Plant J* **74**: 678–689
- 545 **Champagne CEM, Goliber TE, Wojciechowski MF, Mei RW, Townsley BT, Wang K, Paz MM,**
546 **Geeta R, Sinha NR** (2007) Compound leaf development and evolution in the legumes. *Plant Cell*
547 **19**: 3369–3378
- 548 **Coen ES, Romero JM, Doyle S, Elliot R, Murphy G, Carpenter R** (1990) *floricaula*: A homeotic
549 gene required for flower development in *Antirrhinum majus*. *Cell* **63**: 1311–1322
- 550 **Dong Z, Zhao Z, Liu C, Luo J, Yang J, Huang W, Hu X, Wang TL, Luo D** (2005) Floral Patterning

- 551 in *Lotus japonicus*. Plant Physiol **137**: 1272–1282
- 552 **Gaillochet C, Daum G, Lohmann JU** (2015) O Cell, Where Art Thou? The mechanisms of shoot
553 meristem patterning. Curr Opin Plant Biol **23**: 91–97
- 554 **Ganger MT, Girouard JA, Smith HM, Bahny BA, Ewing SJ** (2014) Antheridiogen and abscisic acid
555 affect conversion and ANI1 expression in *Ceratopteris richardii* gametophytes. Botany **93**: 109–
556 116
- 557 **Gourlay CW, Hofer JMI, Ellis THN** (2000) Pea Compound Leaf Architecture Is Regulated by
558 Interactions among the Genes UNIFOLIATA, COCHLEATA, AFILA and TENDRILLESS Plant
559 Cell **12**: 1279–1294
- 560 **Harrison CJ, Morris JL** (2018) The origin and early evolution of vascular plant shoots and leaves.
561 Philos Trans R Soc B Biol Sci **373**: 20160496
- 562 **Hejátko J, Blilou I, Brewer PB, Friml J, Scheres B, Benková E** (2006) *In situ* hybridization technique
563 for mRNA detection in whole mount *Arabidopsis* samples. Nat Protoc **1**: 1939–1946
- 564 **Hellemans J, Mortier G, De Paepe A, Speleman F, Vandesompele J** (2007) qBase relative
565 quantification framework and software for management and automated analysis of real-time
566 quantitative PCR data. Genome Biol **8**: R19
- 567 **Hickok LG, Warne TR, Fribourg RS** (1995) The biology of the fern *Ceratopteris* and its use as a
568 model system. Int J Plant Sci **156**: 332–345
- 569 **Hill JP** (2001) Meristem development at the sporophyll pinna apex in *Ceratopteris richardii*. Int J Plant
570 Sci **16**: 235–247
- 571 **Himi S, Sano R, Nishiyama T, Tanahashi T, Kato M, Ueda K, Hasebe M** (2001) Evolution of
572 MADS-box gene induction by FLO/LFY genes. J Mol Evol **53**: 387–393
- 573 **Hofer J, Turner L, Hellens R, Ambrose M, Matthews P, Michael A, Ellis N** (1997) Unifoliata
574 regulates leaf and flower morphogenesis in pea. Curr Biol **7**: 581–588
- 575 **Hou GC, Hill JP** (2004) Developmental anatomy of the fifth shoot-borne root in young sporophytes of
576 *Ceratopteris richardii*. Planta **219**: 212–220
- 577 **Johnson GP, Renzaglia KS** (2008) Embryology of *Ceratopteris richardii* (Pteridaceae, tribe

- 578 Ceratopterideae), with emphasis on placental development. *J Plant Res* **121**: 581–592
- 579 **Kanrar S, Bhattacharya M, Blake A, Courtier J, Smith HMS** (2008) Regulatory networks that
- 580 function to specify flower meristems require the function of homeobox genes PENNYWISE and
- 581 POUND-FOOLISH in *Arabidopsis*. *Plant J* **54**: 924–937
- 582 **Kato M, Akiyama H** (2005) Interpolation hypothesis for origin of the vegetative sporophyte of land
- 583 plants. *Taxon* **54**: 443–450
- 584 **Kelly AJ, Bonnlander MB, Meeks-Wagner DR** (1995) *NFL*, the tobacco homolog of *floricaula* and
- 585 leafy, is transcriptionally expressed in both vegetative and floral meristems. *Plant Cell* **7**: 225–234
- 586 **Kofuji R, Hasebe M** (2014) Eight types of stem cells in the life cycle of the moss *Physcomitrella*
- 587 *patens*. *Curr Opin Plant Biol* **17**: 13–21
- 588 **Kyozuka J, Konishi S, Nemoto K, Izawa T, Shimamoto K** (1998) Down-regulation of *RFL*, the
- 589 FLO/LFY homolog of rice, accompanied with panicle branch initiation. *Proc Natl Acad Sci U S A*
- 590 **95**: 1979–82
- 591 **Letunic I, Bork P** (2016) Interactive tree of life (iTOL) v3: an online tool for the display and annotation
- 592 of phylogenetic and other trees. *Nucleic Acids Res* **44**: W242–W245
- 593 **Ligrone R, Duckett JG, Renzaglia KS** (2012) Major transitions in the evolution of early land plants:
- 594 a bryological perspective. *Ann Bot* **109**: 851–871
- 595 **Livak KJ, Schmittgen TD** (2001) Analysis of Relative Gene Expression Data Using Real-Time
- 596 Quantitative PCR and the 2– $\Delta\Delta CT$ Method. *Methods* **25**: 402–408
- 597 **MacAlister CA, Bergmann DC** (2011) Sequence and function of basic helix-loop-helix proteins
- 598 required for stomatal development in *Arabidopsis* are deeply conserved in land plants. *Evol Dev*
- 599 **13**: 182–192
- 600 **Maizel A** (2005) The Floral Regulator LEAFY Evolves by Substitutions in the DNA Binding Domain.
- 601 *Science* (80-) **308**: 260–263
- 602 **Maizel A, Busch MA, Tanahashi T, Perkovic J, Kato M, Hasebe M, Weigel D** (2005) The floral
- 603 regulator LEAFY evolves by substitutions in the DNA binding domain. *Science* (80-) **308**: 260–
- 604 263

- 605 **Matasci N, Hung L-H, Yan Z, Carpenter EJ, Wickett NJ, Mirarab S, Nguyen N, Warnow T,**
606 **Ayyampalayam S, Barker M, et al** (2014) Data access for the 1,000 Plants (1KP) project.
607 *Gigascience* **3**: 17
- 608 **Mellerowicz EJ, Horgan K, Walden A, Coker A, Walter C** PRFLL – a *Pinus radiata* homologue of
609 FLORICAULA and LEAFY is expressed in buds containing vegetative shoot and undifferentiated
610 male cone primordia. *Planta* **206**: 619–629
- 611 **Menand B, Yi K, Jouannic S, Hoffmann L, Ryan E, Linstead P, Schaefer DG, Dolan L** (2007) An
612 ancient mechanism controls the development of cells with a rooting function in land plants. *Science*
613 (80-) **316**: 1477–1480
- 614 **Meng Q, Zhang C, Huang F, Gai J, Yu D** (2007) Molecular cloning and characterization of a *LEAFY*-
615 like gene highly expressed in developing soybean seeds. *Seed Sci Res* **17**: 297–302
- 616 **Miki D, Shimamoto K** (2004) Simple RNAi Vectors for Stable and Transient Suppression of Gene
617 Function in Rice. *Plant Cell Physiol* **45**: 490–495
- 618 **Molinero-Rosales N, Jamilena M, Zurita S, Gómez P, Capel J, Lozano R** (1999) FALSIFLORA,
619 the tomato orthologue of FLORICAULA and LEAFY, controls flowering time and floral meristem
620 identity. *Plant J* **20**: 685–693
- 621 **Mouradov A, Glassick T, Hamdorf B, Murphy L, Fowler B, Marla S, Teasdale RD** (1998)
622 NEEDLY, a *Pinus radiata* ortholog of *FLORICAULA/LEAFY* genes, expressed in both
623 reproductive and vegetative meristems. *Proc Natl Acad Sci* **95**: 6537–6542
- 624 **Moyroud E, Kusters E, Monniaux M, Koes R, Parcy F** (2010) LEAFY blossoms. *Trends Plant Sci*
625 **15**: 346–352
- 626 **Moyroud E, Monniaux M, Thévenon E, Dumas R, Scutt CP, Frohlich MW, Parcy F** (2017) A link
627 between LEAFY and B-gene homologues in *Welwitschia mirabilis* sheds light on ancestral
628 mechanisms prefiguring floral development. *New Phytol* **469**–481
- 629 **Nguyen L-T, Schmidt HA, von Haeseler A, Minh BQ** (2015) IQ-TREE: A Fast and Effective
630 Stochastic Algorithm for Estimating Maximum-Likelihood Phylogenies. *Mol Biol Evol* **32**: 268–
631 274

- 632 **Niklas KJ, Kutschera U** (2010) The evolution of the land plant life cycle. *New Phytol* **185**: 27–41
- 633 **Pires ND, Yi K, Breuninger H, Catarino B, Menand B, Dolan L** (2013) Recruitment and remodeling
634 of an ancient gene regulatory network during land plant evolution. *Proc Natl Acad Sci*. **110**: 9571–
635 9576
- 636 **Plackett ARG, Huang L, Sanders HL, Langdale JA** (2014) High-efficiency stable transformation of
637 the model fern species *Ceratopteris richardii* via microparticle bombardment. *Plant Physiol* **165**:
638 3–14
- 639 **Plackett ARG, Rabbnowitsch EH, Langdale JA** (2015) Protocol: Genetic transformation of the fern
640 *Ceratopteris richardii* through microparticle bombardment. *Plant Methods*. **11**: 37
- 641 **Pnueli L, Carmel-Goran L, Hareven D, Gutfinger T, Alvarez J, Ganal M, Zamir D, Lifschitz E**
642 (1998) The self-pruning gene of tomato regulates vegetative to reproductive switching of
643 sympodial mersitems and is the ortholog of CEN and TFL1. *Development* **125**: 1979–1989
- 644 **Proust H, Honkanen S, Jones VA, Morieri G, Prescott H, Kelly S, Ishizaki K, Kohchi T, Dolan L**
645 (2016) RSL Class I Genes Controlled the Development of Epidermal Structures in the Common
646 Ancestor of Land Plants. *Curr Biol* **26**: 93–99
- 647 **Qiu Y-LL, Li L, Wang B, Chen Z, Knoop V, Groth-Malonek M, Dombrovska O, Lee J, Kent L,**
648 **Rest J, et al** (2006) The deepest divergences in land plants inferred from phylogenomic evidence.
649 *Proc Natl Acad Sci U S A* **103**: 15511–15516
- 650 **Rao NN, Prasad K, Kumar PR, Vijayraghavan U** (2008) Distinct regulatory role for RFL, the rice
651 LFY homolog, in determining flowering time and plant architecture. *Proc Natl Acad Sci* **105**:
652 3646–3651
- 653 **Ratcliffe OJ, Bradley DJ, Coen ES** (1999) Separation of shoot and floral identity in *Arabidopsis*.
654 *Development* **126**: 1109–1120
- 655 **Rottmann WH, Meilan R, Sheppard LA, Brunner AM, Skinner JS, Ma C, Cheng S, Jouanin L,**
656 **Pilate G, Strauss SH** (2001) Diverse effects of overexpression of *LEAFY* and *PTLF*, a poplar
657 (*Populus*) homolog of *LEAFY/FLORICAULA*, in transgenic poplar and *Arabidopsis*. *Plant J* **22**:
658 235–245

- 659 **Sakakibara K, Nishiyama T, Deguchi H, Hasebe M** (2008) Class 1 KNOX genes are not involved in
660 shoot development in the moss *Physcomitrella patens* but do function in sporophyte development.
661 *Evol Dev* **10**: 555–566
- 662 **Sano R, Juárez CM, Hass B, Sakakibara K, Iyo M, Banks JA, Hasebe M, Juarez C, Hass B,**
663 **Sakakibara K, et al** (2005) KNOX homeobox genes potentially have similar function in both
664 diploid unicellular and multicellular meristems, but not in haploid meristems. *Evol Dev* **7**: 69–78
- 665 **Sayou C, Monniaux M, Nanao MHH, Moyroud E, Brockington SFF, Thevenon E, Chahtane H,**
666 **Warthmann N, Melkonian M, Zhang Y, et al** (2014) A promiscuous intermediate underlies the
667 evolution of LEAFY DNA binding specificity. *Science* (80-) **343**: 645–648
- 668 **Schmidt A, Schmid MW, Grossniklaus U** (2015) Plant germline formation: common concepts and
669 developmental flexibility in sexual and asexual reproduction. *Development* **142**: 229 LP-241
- 670 **Schultz EA, Haughn GW** (1991) LEAFY, a Homeotic Gene That Regulates Inflorescence
671 Development in Arabidopsis. *Plant Cell* **3**: 771–781
- 672 **Shindo S, Sakakibara K, Sano R, Ueda K, Hasebe M** (2001) Characterization of a
673 FLORICAULA/LEAFY Homologue of *Gnetum parvifolium* and Its Implications for the Evolution
674 of Reproductive Organs in Seed Plants. *Int J Plant Sci* **162**: 1199–1209
- 675 **Souer E, van der Krol A, Kloos D, Spelt C, Bliek M, Mol J, Koes R** (1998) Genetic control of
676 branching pattern and floral identity during Petunia inflorescence development. *Development* **125**:
677 733–742
- 678 **Souer E, Rebocho AB, Bliek M, Kusters E, de Bruin RAM, Koes R** (2008) Patterning of
679 Inflorescences and Flowers by the F-Box Protein DOUBLE TOP and the LEAFY Homolog
680 ABERRANT LEAF AND FLOWER of Petunia. *Plant Cell* **20**: 2033-2048
- 681 **Tanahashi T, Sumikawa N, Kato M, Hasebe M** (2005) Diversification of gene function: homologs
682 of the floral regulator FLO/LFY control the first zygotic cell division in the moss *Physcomitrella*
683 *patens* *Development* **132**: 1727-1736
- 684 **Theissen G, Melzer R** (2007) Molecular Mechanisms Underlying Origin and Diversification of the
685 Angiosperm Flower. *Ann Bot* **100**: 603–619

- 686 **Theißen G, Melzer R, Rümpler F** (2016) MADS-domain transcription factors and the floral quartet
687 model of flower development: linking plant development and evolution. *Development* **143**: 3259–
688 3271
- 689 **Tomescu AMF** (2009) Megaphylls, microphylls and the evolution of leaf development. *Trends Plant
690 Sci* **14**: 5–12
- 691 **Vasco A, Moran RC, Ambrose B** (2013) The evolution, morphology, and development of fern leaves.
692 *Front Plant Sci* **4**: 345
- 693 **Vázquez-Lobo A, Carlsbecker A, Vergara-Silva F, Alvarez-Buylla E, Piñero D, Engström P**
694 (2007) Characterization of the expression patterns of LEAFY/FLORICAULA and NEEDLY
695 orthologs in female and male cones of the conifer genera *Picea*, *Podocarpus*, and *Taxus*:
696 implications for current evo-devo hypotheses for gymnosperms. *Evol Dev* **9**: 446–459
- 697 **Wang H, Chen J, Wen J, Tadege M, Li G, Liu Y, Mysore KS, Ratet P, Chen R** (2008) Control of
698 Compound Leaf Development by FLORICAULA/LEAFY Ortholog SINGLE LEAFLET1 in
699 *Medicago truncatula*. *Plant Physiol* **146**: 1759–1772
- 700 **Weigel D, Alvarez J, Smyth DR, Yanofsky MF, Meyerowitz EM** (1992) LEAFY controls floral
701 meristem identity in *Arabidopsis*. *Cell* **69**: 843–859
- 702 **Weigel D, Nilsson O** (1995) A developmental switch sufficient for flower initiation in diverse plants.
703 *Nature* **377**: 495–500
- 704 **White R, Turner M** (1995) Anatomy and development of the fern sporophyte. *Bot Rev* **61**: 281–305
- 705 **Wickett NJ, Mirarab S, Nguyen N, Warnow T, Carpenter E, Matasci N, Ayyampalayam S,
706 Barker MS, Burleigh JG, Gitzendanner MA, et al** (2014) Phylogenomic analysis of the
707 origin and early diversification of land plants. *Proc Natl Acad Sci* **111**: E4859–E4868
- 708 **Wreath S, Bartholmes C, Hidalgo O, Scholz A, Gleissberg S** (2013) Silencing of EcFLO, A
709 FLORICAULA/LEAFY Gene of the California Poppy (*Eschscholzia californica*), Affects Flower
710 Specification in a Perigynous Flower Context. *Int J Plant Sci* **174**: 139–153
- 711 **Yang T, Du MF, Guo YH, Liu X** (2017) Two LEAFY homologs ILFY1 and ILFY2 control
712 reproductive and vegetative developments in *Isoetes L*. *Sci Rep* **1**: 225

- 713 Yip HK, Floyd SK, Sakakibara K, Bowman JL (2016) Class III HD-Zip activity coordinates leaf
714 development in *Physcomitrella patens*. *Dev Biol* **419**: 184–197
- 715 Zhao W, Chen Z, Liu X, Che G, Gu R, Zhao J, Wang Z, Hou Y, Zhang X (2017) CsLFY is required
716 for shoot meristem maintenance via interaction with WUSCHEL in cucumber (*Cucumis sativus*).
717 *New Phytol* **218**: 344–356
- 718 Zhao Y, Zhang T, Broholm SK, Tähtiharju S, Mouhu K, Albert VA, Teeri TH, Elomaa P (2016)
719 Evolutionary Co-Option of Floral Meristem Identity Genes for Patterning of the Flower-Like
720 Asteraceae Inflorescence. *Plant Physiol* **172**: 284–296
- 721

SUPPLEMENTAL FIGURES

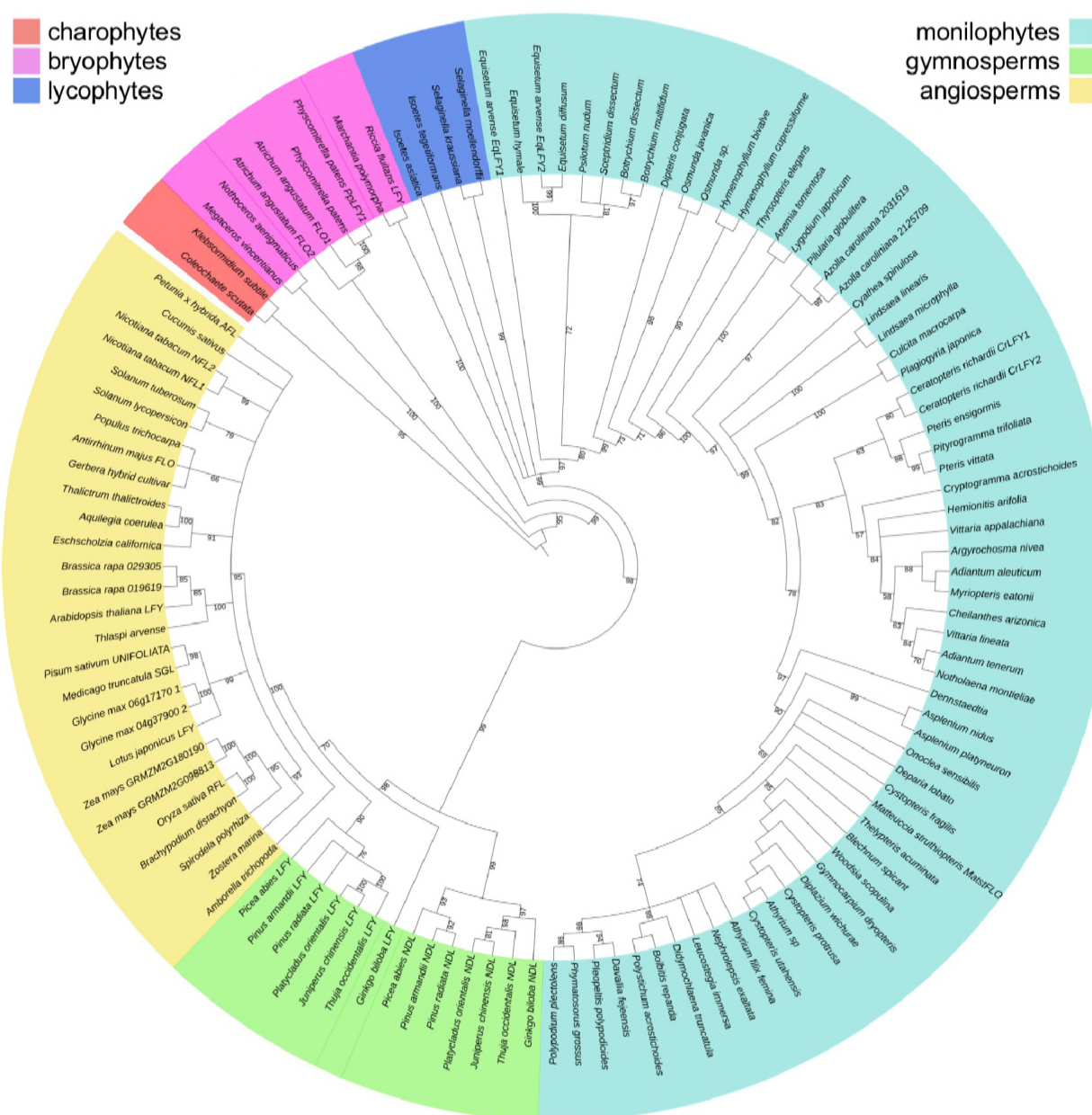


Figure 1-figure supplement 1. Phylogenetic relationships between *LEAFY* sequences reflect established relationships within vascular plant lineages. Inferred phylogenetic tree from maximum likelihood analysis of 120 LFY sequences sampled from across extant land plant lineages (liverworts, mosses, hornworts, lycophytes, monilophytes i.e. ferns and allies, gymnosperms, angiosperms) including algal (charophyte) sequences as an outgroup. Bootstrap values are given for each node. Sequences belonging to each lineage are denoted by different colours, as shown. The higher-order topology between vascular plant lineages (lycophytes, monilophytes, gymnosperms and angiosperms) is consistent with expected relationships; a gene duplication event resulting in *LFY* and *NEEDLY* clades in gymnosperms has been identified previously (Sayou et al., 2014); and relationships between bryophyte lineages are consistent with differences in the LFY DNA binding site preference, where hornworts and mosses each differ from the preferred site shared by liverworts and vascular plants (Sayou et al., 2014).

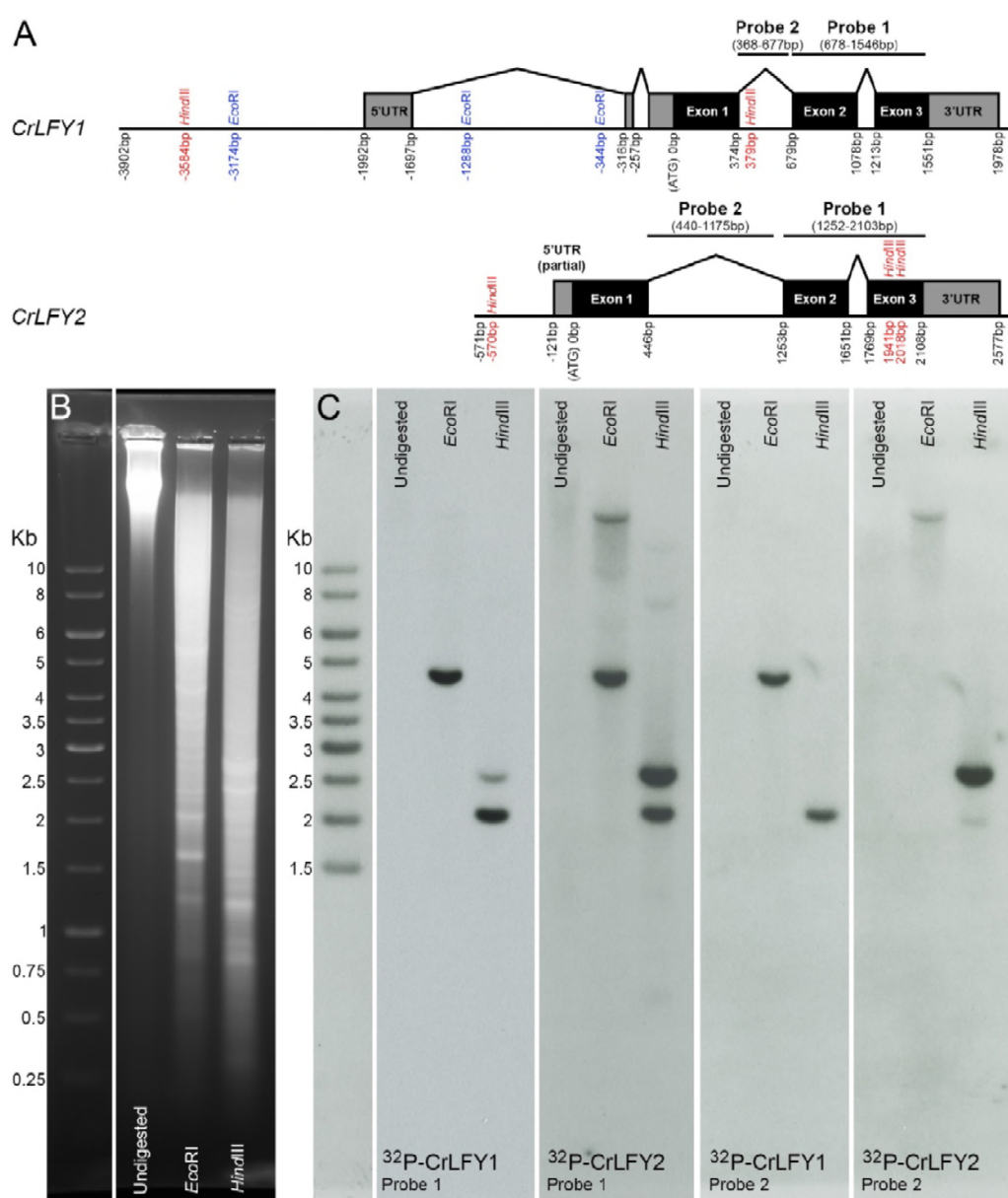


Figure 1-figure supplement 2. The *Ceratopteris* genome contains only two copies of *LFY*.

A. Deduced gene structure of *CrLFY1* and *CrLFY2* loci. All positions marked are given relative to the ATG start codon. Hybridization probes used in DNA gel blot analysis and relevant restriction sites (*Eco*RI, *Hind*III) are marked. *CrLFY1* probe 1 (868bp) and *CrLFY2* probe 1 (851bp) share 79% sequence similarity and hybridize to exons 2+3 of each gene (comprising the conserved LFY DNA binding domain). As such, both probes should hybridize to all members of the *LFY* gene family. *CrLFY1* probe 2 (309bp) and *CrLFY2* probe 2 (735bp) hybridize to intron 1 of each gene copy and share no significant sequence similarity. As such, each probe is expected to hybridize to the specific gene copy. B, C. Gel blot analysis of wild-type genomic DNA, digested with *Eco*RI or *Hind*III, electrophoresed on an ethidium bromide stained gel (B), blotted to nylon membrane and hybridized against different probes (C) as described in (A). *Eco*RI digestion was predicted to generate single hybridizing fragments for both *CrLFY1* and *CrLFY2*, each spanning both probes with minimum expected fragment sizes of ~2.0kb and ~3.1kb, respectively. *Hind*III digestion was predicted to generate a single *CrLFY1* hybridizing fragment recognized by both probes with a minimum size of ~1.6kb. *Hind*III digestion was predicted to generate a *CrLFY2* fragment of ~2.5kb hybridizing to probes 1 and 2, a separate fragment with a minimum size of 559bp overlapped by 85bp of probe 1 (and so potentially undetectable) plus an undetectable fragment of 11bp. The hybridization patterns observed (C) are consistent with these predictions, with the exon probes cross-hybridizing to predicted fragments of both gene copies (but not to any additional gene fragments) and the intron probes primarily hybridizing to the respective specific gene copy.

727

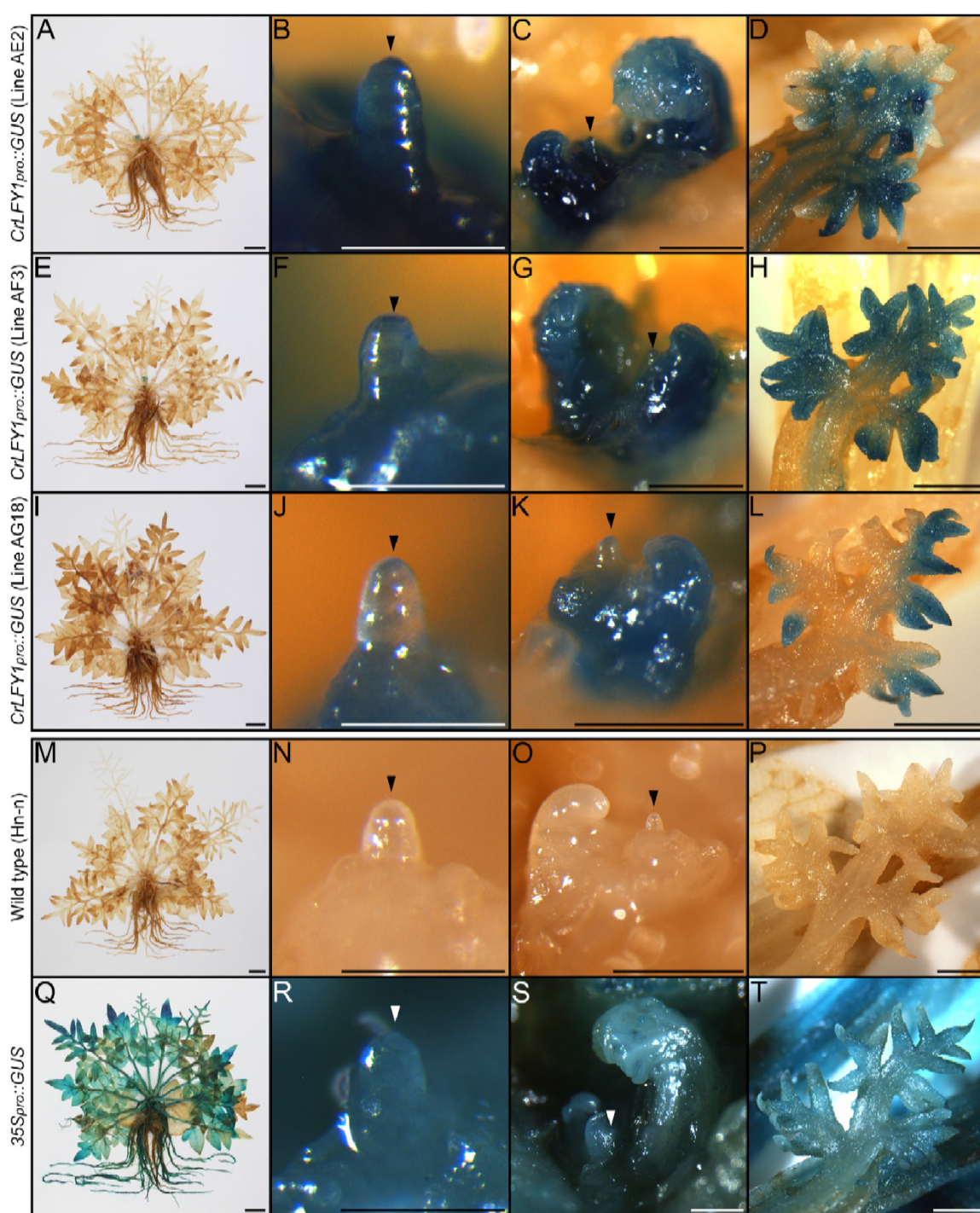


Figure 4-figure supplement 1. *CrLFY1_{pro}::GUS* expression patterns are similar in *Ceratopteris* shoots before and after reproductive phase change. GUS activity detected as blue staining in sporophytes producing fronds with spore-bearing morphology (narrowing and elongation of pinnae) from three independent *CrLFY1_{pro}::GUS* transgenic reporter lines (A-L; 110-124 DAF), negative wild-type controls (M-P; 113 DAF) and positive *35S_{pro}::GUS* controls (Q-T; 110 DAF). Staining patterns were consistent between the three independent *CrLFY1_{pro}::GUS* transgenic lines (A, E, I), and were similar to those seen at 60 DAF (Figure 4 C, H, M). GUS activity was observed throughout the shoot apex (B, F, J) and in recently-emerged frond primordia (C, G, K). Activity persisted later in frond development, becoming restricted to developing pinnae (D, H, L). GUS staining was lost from fronds prior to maturity (A, E, I). No endogenous GUS activity was detected in wild-type controls (M-P) whereas activity was detected throughout all non-senescent tissues in the *35S_{pro}::GUS* line (Q-T).

728

729

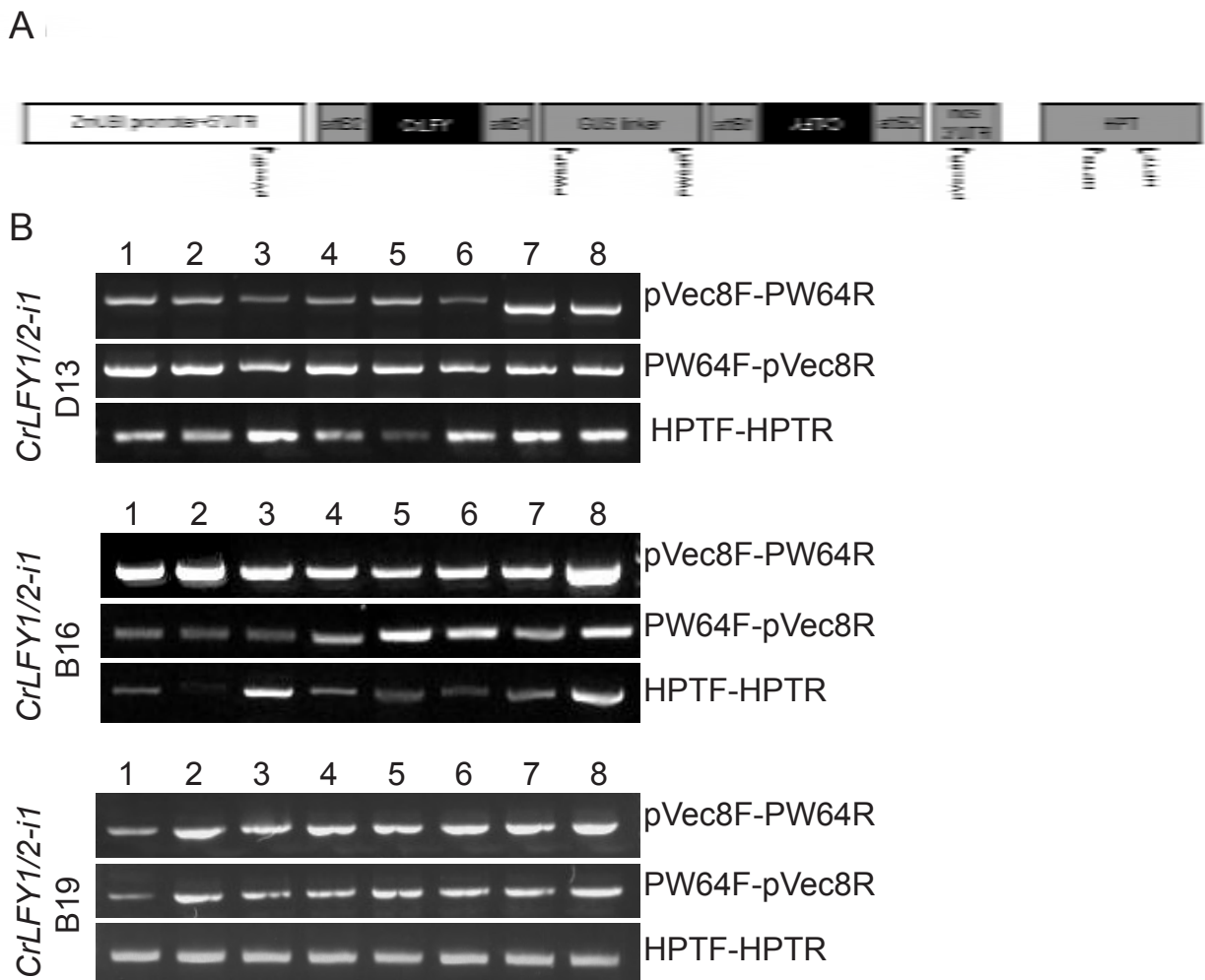


Figure 6-figure supplement 1. Gametophytes exhibiting developmental arrest were transgenic. A. Generalized schematic of *CrLFY* RNAi T-DNA with the relative position of primers used in genotyping PCR marked. Primer sequences and expected PCR product sizes for each *CrLFY* RNAi construct are given in **Table S6-8**. B. Genotyping PCR was conducted on DNA extracted from single gametophytes exhibiting developmental arrest at 10 DPS in three *ZmUbi_{pro}::CrLFY1/2-i1* lines. DNA from all arrested individuals amplified positive bands for the two hairpin arms (pVec8F-PW64R & PW64F-pVec8R) and for the hygromycin resistance marker (HPTF-HPTR).

730

731

732

733

734

735

736

737 **SUPPLEMENTARY FILES**

738 **Supplementary File 1.** Additional LFY sequences included in phylogenetic analysis.

739 **Supplementary File 2.** Alignment of all LFY amino acid sequences used in phylogenetic analysis.

740 **Supplementary File 3.** Alignment of LFY amino acid sequences used in phylogenetic analysis (ferns
741 only).

742 **Supplementary File 4.** Statistical comparison of *CrLFY* transcript levels between different ontogenetic
743 stages

744 **Supplementary File 5.** Design and validation of *CrLFY**I_{pro}::GUS* transgenic lines.

745 **Supplementary File 6.** Design and validation of *CrLFY* RNAi transgenic lines.

746 **Supplementary File 7.** Gel blot analysis and *in situ* hybridization probe design.

747 **Supplementary File 8.** Summary of published reports of LFY function in a range of angiosperm
748 species.

749